Proceedings of the MCEER Workshop on Ground Motion Methodologies for the Eastern United States

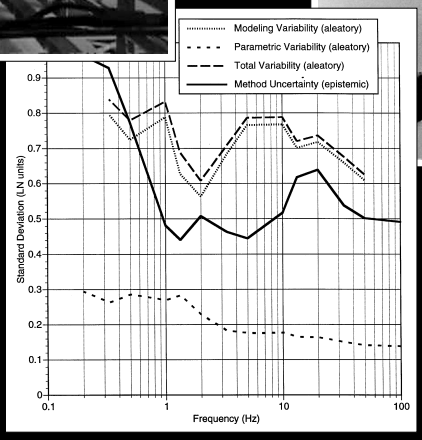

Edited by

Norman Abrahamson
Engineering Seismology Consultant
152 Dracena Avenue
Piedmont, California 94611-3903

Ann Becker
Engineering Seismology Consultant
2724 Meadow Drive
Lawrence, Kansas 66047

MCEER
MULTIDISCIPLINARY CENTER FOR EARTHQUAKE ENGINEERING RESEARCH
A National Center of Excellence in Advanced Technology Applications

ISSN 1520-295X

Technical Report MCEER-99-0016
August 11, 1999

This workshop was held at the Sheraton Four Points Hotel, Memphis, Tennessee, and was supported by the Federal Highway Administration under contract number DTFH61-92-C-00106.

NOTICE

This report was prepared by the Multidisciplinary Center for Earthquake Engineering Research (MCEER) through a contract from the Federal Highway Administration. Neither MCEER, associates of MCEER, its sponsors, the Federal Highway Administration, nor any person acting on their behalf:

a. makes any warranty, express or implied, with respect to the use of any information, apparatus, method, or process disclosed in this report or that such use may not infringe upon privately owned rights; or

b. assumes any liabilities of whatsoever kind with respect to the use of, or the damage resulting from the use of, any information, apparatus, method, or process disclosed in this report.

Any opinions, findings, and conclusions or recommendations expressed in this publication are those of the author(s) and do not necessarily reflect the views of MCEER or the Federal Highway Administration.

Cover Credits

Left photograph courtesy of the Missouri Department of Transportation.

Right photograph courtesy of HNTB Corporation.

Proceedings of the MCEER Workshop on Ground Motion Methodologies for the Eastern United States

Held at
Sheraton Four Points Hotel
Memphis, Tennessee
October 16-17, 1997

Edited by
Norman Abrahamson[1] and Ann Becker[2]

Publication Date: August 11, 1999

Technical Report MCEER-99-0016

Task Number 106-F-5.4.2

FHWA Contract Number DTFH61-92-C-00106

1 Engineering Seismology Consultant, Piedmont, California
2 Engineering Seismology Consultant, Lawrence, Kansas

MULTIDISCIPLINARY CENTER FOR EARTHQUAKE ENGINEERING RESEARCH
University at Buffalo, State University of New York
Red Jacket Quadrangle, Buffalo, NY 14261

Table of Contents

Table of Contents (cont'd)

** Appendices B through J are provided on MCEER's web site at http://mceer.buffalo.edu.*

List of Illustrations

List of Illustrations (cont'd)

List of Tables

SECTION 1
INTRODUCTION

In October 1997, the Multidisciplinary Center for Earthquake Engineering Research (formerly the National Center for Earthquake Engineering Research) and the Federal Highway Administration (FHWA) sponsored a two-day workshop, *Ground Motion Methodologies for the Eastern United States*, to evaluate ground motion modeling methods applicable in the eastern U.S. The predictive methods were to be assessed for their ability to produce time histories appropriate for use in engineering applications. The intent of the workshop was not to rank various modeling methodologies, but rather to evaluate the state-of-the-art for strong ground motion prediction in the region and the variability of time histories from different modeling methods. Further, the workshop served to introduce the participants to the concept of formal model validation and thence application to develop synthetic motions. This focus on practicality responded to the user community's need to evaluate the credibility of synthetic time histories developed for specific projects and the lack of criteria on which to base these evaluations.

Two issues were paramount in the evaluation of the time histories: the peak amplitudes of the ground motion and the non-stationary character of the time history. The models were assessed against the following measures:

- the ability of the methods to predict the amplitude of the ground motion (median and variability) expressed as elastic response spectra;
- their ability to define the non-stationary characteristics of the time history expressed as duration of the acceleration, velocity and displacement;
- whether synthetic time histories require further scaling and, if so, what the scaling rules are;
- what means can be used to evaluate synthetic time histories to ensure they are reasonable.

Ultimately, the workshop resulted in recommendations as to the seismological community's ability to predict absolute levels of expected shaking and to judge whether synthetic motions required subsequent modification.

1.1 User Needs

The engineering community involved in the seismic assessment of eastern U.S. (EUS) facilities looks to the seismological community to define ground motion time histories for seismic evaluation of structures. In previous highway projects, time histories developed by different groups have been significantly different in both amplitude and waveform. The engineering community requires criteria to evaluate the adequacy of synthetic ground motions, whether defined by time histories or response spectra, or other ground motion characteristics. They also require guidance regarding use of finite fault modeling for near-fault motions. Finally, they require a cost-effective approach to develop motions for standard application.

Because of the scarcity of recorded EUS strong ground motions for comparisons, the engineering community lacks measures against which they may judge the attributes of synthetic time histories. Currently available attenuation relations provide estimates of the response spectral values, but for evaluating time histories, estimates of the peak ground velocity and peak ground displacement are also needed. Additionally, measures of non-stationarity are needed to check the synthetic time histories: acceleration (velocity, and/or displacement) duration, and/or the slope of a Husid plot for the motion, and a recommendation on one- or two-sided displacement histories.

Practitioners also need cost-effective methods to develop ground motions for use in typical applications. Site-specific modeling can be costly and generally is warranted only for the analysis of critical facilities. A standard library of time histories for EUS earthquakes is needed for use in engineering evaluations. This library should include well documented motions for a few representative cases and guidelines on acceptable methods of scaling them.

1.2 Validation and Simulation Studies

The goal of the NCEER/FHWA workshop was not to set target spectra or other acceptability criteria, but rather to evaluate synthetic time histories resulting from various predictive models. The workshop focus on methods of predicting strong ground motion was the first step in addressing the needs of the engineering community by assessing the capabilities of available numerical simulation procedures. An element of this effort consists of a validation exercise for each modeling method to check model calibrations and test parameter sensitivities. A suite of simulations from each method is needed to estimate the median ground motion and the variability.

This approach has been adopted in several recent studies including the 1990 Diablo Canyon Long Term Seismic Program (LTSP; an in-depth evaluation of the seismic hazard and risk at the plant), the 1993 EPRI study of EUS ground motions, the 1995 Southern California Earthquake Center study of scenario earthquakes in southern California, the 1996 Yucca Mountain (Nevada) study of scenario earthquakes, and the 1997 Yucca Mountain probabilistic seismic hazard analysis. The NCEER/FHWA workshop was constructed using what was learned from these studies in terms of how to organize the exercises (necessary constraints), how to validate the models, and how to compare the results. Several participants in the workshop also contributed to one or more of the previous studies.

The validation is intended to evaluate how well the models can predict ground motion from a past earthquake. Each modeler estimates ground motion for a recorded earthquake using source, path, and site parameters that are appropriate for the events and optimizing other model parameters to provide the best data fit. Comparisons of the predicted ground motions with the recorded motions results in model misfits to the data, an important element of the uncertainty in future estimates of ground motion in postulated earthquakes. Although comparisons against recordings from more than one earthquakes is needed to validate a model, a single earthquake

validation exercise was performed in this workshop to demonstrate the concept and to provide a rough evaluation of the adequacy of the models.

In the simulation exercise, the numerical models are used to predict ground motion for a future earthquake. Select parameters (such as event magnitude, fault geometry, station locations, site or path parameters) are fixed and multiple realizations are performed which randomize event-specific parameters, which were optimized in the validation exercise. The predicted ground motions from the alternative modeling methods are summarized by the median ground motion and standard deviation (variability)

1.3 Treatment of Variability

The modeling methods used by the different groups include different sets of source, path, and site parameters. To track the variability of the model prediction, each model parameter must be declared as "fixed" or "event-specific." Event-specific parameters are optimized to the best value for each past earthquake considered in the validation exercise. Since the event-specific parameters are unknown for future earthquakes, they must be randomized in the scenario simulations. Fixed model parameters are not randomized in the scenario simulations because the effect of the variability of these parameters is captured in the misfits to the recorded data in the validation exercise (assuming enough earthquakes are included in the validation to represent the variability).

For example, one model may assume that the stress-parameter of the sub-events are constant for all earthquakes, whereas another model may assume that the stress-parameter is event-specific. The first model may accurately predict the median ground motion from a suite of past earthquakes (e.g., it is unbiased) but it will probably have a poorer fit to the individual earthquake than the second model. When predicting ground motions for a future earthquake, the first model would keep the sub-event stress-parameter fixed, but the second model would have to specify a distribution of the stress-parameter and then sample the distribution for a suite of simulations.

This leads to two types of variability of the predicted ground motions. The variability from the misfit of the predicted ground motions to recorded ground motions from past earthquakes is called "modeling variability." The modeling variability reflects the limitations of the model to predict the ground motion even when all of the event-specific parameters are known. In the context of the model, these variations are unexplainable randomness. The modeling variability can only be computed by comparing predicted ground motions to observed ground motions.

The variability due to variations in event-specific parameters for future earthquakes is called "parametric variability." This represents the variability of the ground motion that results from varying the event-specific source parameters. In contrast to the modeling variability, this source of variability is understood. The parametric variability is computed using multiple realizations of the simulation process that sample the range of event-specific parameters.

To compare the variability of ground motion predictions from alternative models, it is important to keep track of both the modeling variability and the parametric variability. The total variability is the combination of the modeling and parametric variability. In general, as more event-specific parameters are included in the model, the modeling variability is shifted to parametric variability. Whether the total variability goes up or down as more event-specific parameters are included depends on how well the distribution of the event-specific parameters for the events used in the validation agrees with the distribution assumed for those parameters in the simulations. If a large enough sample of events is used in the validation, then the total variability is unlikely to change as more event-specific parameters are used: the reduction in the modeling variability is offset by a corresponding increase in the parametric variability. There is, however, an advantage to shifting modeling variability to parametric variability: the cause of the parametric variability is understood; whereas, the cause of the modeling variability is not explicitly understood.

The validation has two purposes. First, it is intended to determine if the model predictions are unbiased on average. Second, it provides an estimate of the modeling variability.

In this workshop, we have only used a single event in the validation exercise. A single event is not sufficient to evaluate the model bias on average, nor does it provide an accurate estimate of the modeling variability. A full validation was beyond the scope of the workshop. Some of the models have been validated for a larger number of events in previous studies. When available, we have included these more comprehensive validation results in these proceedings in addition to the single event validation results.

1.4 Treatment of Uncertainty

The variability discussed above is called "aleatory" variability. It represents variability that is considered to be random. In addition to aleatory variability, there is "epistemic" uncertainty. Epistemic uncertainty is uncertainty due to insufficient data (lack of information). In ground motion modeling, epistemic uncertainty results from uncertainty in the distributions of parameter values.

For a fixed model parameter, there is epistemic uncertainty on the best fixed value due to the small number of earthquakes used in the validation. For an event-specific model parameter, there is epistemic uncertainty in the probability density function for the parameter. Using the example of sub-event stress parameter again, if it is a fixed parameter, there is epistemic uncertainty in the best average value due to the small number of earthquakes used in the validation. If it is an event-specific parameter, then there is uncertainty both in the median value and standard deviation used to represent the range of sub-event stress parameter values for future earthquakes.

In previous studies, epistemic uncertainty has not typically been assessed for individual models, but rather it has been assessed by comparing the median and variability of ground

motions from alternative credible models. (Here, credible implies that the model has an acceptably small model bias in the model validation.) This approach also incorporates the uncertainty in the basic underlying physical model used in the numerical process.

Because epistemic uncertainty is due to lack of data, as more data become available, epistemic uncertainty will be reduced. The additional data will provide constraints on the distribution of event-specific parameters and the alternative modeling methods should produce more similar results as they are modified based on additional earthquake recordings

SECTION 2
GROUND MOTION MODELING METHODS

Nine scientists experienced in ground motion modeling were invited to participate in the workshop. They were asked to both validate their models and estimate motions for the earthquake scenario. As part of the exercise, both median values and the variabilities in ground motions were to be estimated. Several of the simulation methods considered here have previously been used to obtain ground motions for engineering projects. These typically have been calibrated against recordings from a number of eastern and/or western U.S. events. Other participants' methods are more experimental in nature and have not yet been calibrated against a large number of past earthquakes.

2.1 Selection of Modeling Methods

A set of criteria was developed to aid in the selection of modeling methods and participating modelers. The criteria included:

- The methods are amenable to evaluation of parameter sensitivity and ground motion uncertainty.
- The methods are appropriate for application in the EUS.
- The modelers are experienced in the field.
- The modelers are familiar with ground motion modeling for engineering purposes.

When possible, modelers who had previously applied their models on MCEER projects were given preference in the selection process.

Of the range of modeling approaches available for application, nine individuals familiar with various methods were asked to participate. The nine selected and the methods they applied were:

- John Anderson (Univ. Nevada, Reno) - Composite Fractal Source Method
- Gail Atkinson (Carleton Univ.) - Stochastic Model with Empirical Source Spectrum
- Shyh-Jeng Chiou (Geomatrix Consultants) Hybrid Kinematic Source Model
- Steve Horton (Lamont-Doherty Geological Observatory)
- Larry Hutchings (Lawrence Livermore National Laboratory) - Empirical and Analytical Green's Function Method
- Dan O'Connell (Bureau of Reclamation) - Isochron Method
- Apostolos Papageorgiou (Rensselaer Polytechnic Inst.) - Specific Barrier Method
- Walt Silva (Pacific Engineering & Analyses) - Stochastic Method with ω^2 Sub-events
- Paul Somerville (Woodward-Clyde Federal Services) - Broadband Green's Function Method

Ultimately, eight of the invited participants contributed in some manner to the study (all excepting Dr. Horton). The eight simulation methods are described in the following section. Three participants limited their participation to a varying extent: Dr. Hutchings performed the

validation exercise only; Dr. Papageorgiou briefed the other participants on his modeling method and did not contribute to the validation or scenario exercises; Dr. Somerville did not perform the validation exercise as his model had previously been calibrated against the Saguenay event.

2.2 Description of Simulation Methods

All the various modeling methods applied may be considered as 'physically-based' in that they are based on seismological models of the source, wave propagation, and site effects. All of the models used a finite-source in which the motions for the desired event are formed by summing the ground motions from a number of smaller sub-events distributed on a rupture plane. Taken together, the models represent a broad range of technical approaches to simulating ground motions. The inherent assumptions (and the models) of the sub-events and the manner in which the sub-events combine to build the mainshock differ in each model. They differ in the manner in which seismic slip is distributed and released on the fault surface, in their assumptions of wave propagation, in their assumptions of site response, and in their overall level of complexity. Nevertheless, they accommodate the essential aspects of seismic energy being generated by a finite source and propagated along a path to a recording site. The simulation methods are briefly discussed below.

2.2.1 Composite Fractal Source Method

Dr. John Anderson and Shen-Der Ni apply the composite source model. The source model was developed by Zeng et al. (1994) and comprises a superposition of circular sub-events across a fault area, with the sub-event radii distributed according to a power law (Frankel, 1991). The sub-events are modeled as Brune pulses (ω^{-2} spectra roll-off). The stress drop of the sub-events is constant over the fault plane except at shallow depths, where it decreases to zero.

Wave propagation is accommodated using synthetic Green functions generated from the generalized reflection and transmission coefficients method for a layered earth (Luco and Apsel, 1983) and wave scattering based on isotropic scattering theory. The site response may be modeled either by a kappa filter with crustal factors (Su et al., 1996) or by a site-specific velocity profile with Q; the former was used in this study.

2.2.2 Stochastic Model with Empirical Source Spectrum

A stochastic finite-fault model was applied by Drs. Gail Atkinson and Igor Beresnev (Beresnev and Atkinson, 1997, 1998a). A rectangular fault plane is assumed. The rupture initiates at the hypocenter and propagates radially from it. The velocity of rupture propagation is assumed to equal 0.8 times the shear wave velocity. The fault plane is subdivided into rectangular elements (sub-faults); each sub-fault is triggered as the rupture reaches its center. The number of sub-fault triggerings is adjusted to conserve the total moment of the modeled earthquake. Inhomogeneous slip distribution on the target fault is allowed. The sub-fault acceleration time histories are propagated to the observation point using empirical distance-dependent duration,

geometric attenuation, and attenuation (Q) models. The "kappa" high-cut filter is applied. The total radiated field is obtained by summing contributions from all sub-faults.

The source spectrum for each sub-fault is obtained by multiplying the ω^2 spectral shape by the normalized spectrum of a limited-duration Gaussian noise. The corner frequency of the ω^2 spectrum and the sub-fault moment are derived from the sub-fault size. The amplitude of high frequency radiation is controlled by the radiation-strength factor, which is proportional to the maximum slip velocity on the fault. The frequencies modeled are 0.1 to 50 Hz.

2.2.3 Hybrid Kinematic Source Model

Dr. Chiou's simulation procedure uses a hybrid source model and broadband Green's functions for a layered crust. The source model is a hybrid model in the sense that the slip amplitude at small wavenumber follows a pre-specified spatial distribution, while at large wavenumber it follows a power law decay of κ^2 (κ is the wavenumber) (Herrero and Bernard, 1994; Joyner, 1995) with a randomly assigned phase. For example, in the validation exercise, the Saguenay source is represented as the superposition of a stochastic slip distribution on top of the smoothly varying slip distribution obtained by modeling the recorded strong motion records (Hartzell and others, 1994).

Following Bernard et al. (1996), the source time function has a scale-dependent rise time that corresponds to a propagating source pulse with a finite spatial width. Furthermore, a scale-dependent rake angle is also adopted so that the angle of the large wavenumber slip component is randomized, while the angle of the small wavenumber slip component follows a specified value (78° for the Saguenay earthquake and 90° for the simulation exercise).

The theoretical Green's function is computed up to 30 Hz by the method of generalized reflectivity (Luco and Apsel, 1983; Zeng and Anderson, 1994). Random rake angle and isotropic wave scattering are also included in the simulation to enhance the motions on the near nodal components (Zeng et al., 1995).

2.2.4 Empirical and Analytical Green's Function Method

Dr. Lawrence Hutchings, together with Dr. Steven Jarpe, has developed an exact solution to the representation relation for finite rupture that utilizes either empirical or synthetic Green's functions (Hutchings and Wu, 1990; Hutchings 1991, 1994; Jarpe and Kasameyer, 1996). In the MCEER study, recordings of small earthquakes are used as empirical Green's functions for frequencies of 0.5 to 25.0 Hz and analytical calculations are used to provide synthetic Green's functions for frequencies between 0.05 and 0.5 Hz. The entire wavetrain is synthesized for three components. Linear ground motions were developed as may be expected at the modeled rock outcrops.

The Kostrov slip rupture model with healing discussed by Hutchings (1991, 1994) is used for finite rupture. This results in a continuous rupture over fault segments with variable slip amplitude, but constant stress drop. A percentage of roughness can be added to the model that results in portions of high stress drop, and large asperities can be included that have relatively high stress drop. The rupture model includes rupture over the entire portion of the segment with higher slip amplitudes occurring within asperities.

In the study, empirical Green's functions were not available from the sites to be modeled, or along the source to be modeled. Instead, recordings from small earthquakes obtained at nearby weak-motions recorders were used to obtain empirical Green's functions. These were interpolated to have been located from the sites used in the modeling.

2.2.5 Isochron Integration with Empirical Scattering Functions

The isochron method was used by Dr. Dan O'Connell. The kinematic model consists of self-similar effective stresses with high effective-stress circular asperities imbedded in a fault with randomized rupture and healing velocities. Variable effective-stress asperities provide the dominant short period component of seismic energy. On the modeled surface, perimeter transition regions smoothly decrease effective stresses from the asperity interiors to fault background regions and also allow for abrupt changes in local rupture and healing velocities. Rupture and healing velocities and effective stresses are independently specified for asperity interiors. Asperities are allowed to heal from their transition regions inward.

Background regions of the fault that are far from healing boundaries (fault edges) are permitted to have substantially longer rise times than in the fault interior. This allows for quite heterogeneous distributions of rise time on the fault, consistent with the results of Mikumo and Miyatake (1987, 1993) and Fukuyama and Mikumo (1993). Short rise times in the asperities provide large amplitude short period radiation consistent with Heaton's (1990) observation of relatively short rise times for rupture models of large earthquakes. Longer rise times in the lower effective stress background region provide sufficient additional seismic moment to produce total moments consistent with observed broadband magnitudes (Horton, 1996). If short rise times are assumed everywhere on a fault, then the asperities are required to provide most of the moment and estimated effective stresses are extremely high. The variable rise-time parameterization provides a means to explain low and high frequency observations of large earthquakes, but requires less extreme effective stresses in the asperities than the constant rise time model.

Isochron integration was used to calculate synthetic seismograms by assuming that all significant radiation from the fault consists of first S-wave arrivals and that all seismic radiation from a fault can be described with rupture and healing isochrons. Nine microearthquakes, recorded in the Transverse Ranges of southern California, were used to derive site-specific scattering functions solely from the observed waveforms. Wave-shaping filters, W, were calculated (Yilmaz, 1987) to annihilate 2.5 sec to 3 sec waveform windows that immediately

follow the first one to two cycles of the direct S-waves. The site-specific scattering function, *S*, is the inverse of *W*. To approximate the complexity of observed microearthquake waveforms noted in southern California, one of the nine scattering functions was selected at random at each integration position along an isochron and the appropriate radiation pattern, free-surface correction, geometric spreading, and take-off angle were applied to produce a band-limited site-specific Green function. Calculations were limited to a maximum frequency of 10 Hz.

2.2.6 Specific Barrier Method

The specific barrier method is followed by Dr. Apostolos Papageorgiou. The first step in strong motion prediction for a tectonic region like the eastern U.S., with an extremely limited recorded strong motion database, is to propose a physical model which, when calibrated against the very limited available data, would allow one to extrapolate from moderate events (such as the Saguenay earthquake) to large events (such as the scenario event). In other words, it is necessary to establish scaling laws for the various source parameters, based on the proposed model, so that one can predict/model the motion of large events for which there are no data.

The specific barrier model provides a complete framework for strong motion prediction, including scaling of source parameters, that may be used to specify realistic slip distributions on the fault plane (e.g., using the spectral representation technique of Shinozuka), as well as source spectra and their scaling law. Furthermore, the framework of the specific barrier model is very versatile, allowing one to predict strong ground motion using the engineering (stochastic) approach (e.g., a la Boore, 1983), or the seismological (kinematic modeling) approach using synthetic Green functions (e.g., a la Zeng et al., 1994), or a hybrid of empirical and synthetic Green functions (e.g., a la Somerville, 1993).

Dr. Papageorgiou uses the model of a circular crack to represent sub-events in the specific barrier model. The model is optimized by using two stress drops: a global value for the rupture as a whole and a local value for the sub-event. The source model superposes point sources positioned at the centroids of the isochron patterns for each recording site. Effectively, this assumes that the barrier crack boundaries are approximated by the isochrons and it ultimately represents an optimization of the hypocenter locations.

2.2.7 Stochastic Method with ω^2 Sub-events

The stochastic finite-fault method with ω^2 sub-events is practiced by Dr. Walt Silva of Pacific Engineering & Analysis. The method is an extension of the point-source stochastic method to the finite-fault case using the band-limited white noise (BLWN) model with random vibration theory (RVT).

The fault rupture plane is discretized into a number of equal size sub-fault regions. The radiation pattern is described by a constant, which is the average factor for all of the sub-fault regions. Different values of the slip are assigned to each sub-fault element to incorporate

asperities into the model. Empirical models are used to estimate the rise times of the mainshock and sub-events. Heterogeneity of the source process is accommodated by randomizing the location of the sub-events within each sub-fault element and by randomizing the sub-event rise time.

The path effect is approximated using Q(f) and geometrical attenuation computed by raytracing from each sub-fault to the site. The crustal amplification is computed from the EPRI mid-continent model. Site effects are modeled by a kappa filter and an equivalent-linear model is incorporated into the finite-fault code to accommodate nonlinear site response (Silva and Lee, 1987).

RVT is used to estimate the response spectra to yield more stable estimates of the spectral values than the set of time histories provides. To generate time histories, the Fourier phase spectrum of the sub-event is represented empirically using a small (M 5.0) Eastern North America event recorded at a rock site at a close distance. The sub-event time history is estimated using the empirical phase with the ω^2 amplitude spectrum for the particular sub-event. This is then convolved with a spike seismogram developed from the rupture times and amplitudes of each sub-event. All validations have been done accommodating site conditions using generic rock or soil profiles and equivalent linear soil response.

2.2.8 Broadband Green's Function Method

The broadband Green's function is practiced by Dr. Paul Somerville of Woodward-Clyde Federal Services. This method combines two different procedures for the low frequency (less than 1 Hz) and high frequency (greater than 1 Hz) portions of the ground motion. At low frequency, theoretical source models are used including the theoretical radiation pattern; at high frequencies, empirical source functions are used that incorporate the radiation pattern empirically.

For both procedures, the fault rupture plane is discretized into a number of equal size sub-fault regions. Different values of the slip are assigned to each sub-fault element to incorporate asperities in the model. Empirical models are used to estimate the rise time of the mainshock. The sub-event rise time of the event from which the empirical source functions are derived is estimated independently. Heterogeneity of the source process is modeled by randomizing the selection of the empirical source functions and by randomizing the location of the sub-events within each sub-fault element.

Wave propagation is accommodated using synthetic Green's functions generated using the frequency-wavenumber integration for the long-period procedure and using generalized rays (direct and first multiple) for the high-frequency procedure. Linear site response is incorporated in the empirical source functions which have been corrected as necessary for eastern U.S. site kappa.

Table 2-1: Summary of Modeling Approaches

Participant	Source Model	Path Effect	Scattering	Site Effect
Anderson/Ni	• Composite finite model; superposition of circular sub-events with fractal distribution	• 1-D Green functions • Scattering	• Model parameter	• Kappa
Atkinson/ Beresnev	• Finite discretized into sub-faults • Inhomogeneous slip distribution • Sub-faults have stochastic ω^2 spectrum • Constant rupture velocity, randomized rise time, average radiation pattern	• Empirical EUS geometric spreading and Q models	• Empirical EUS distance-dependent duration model	• Kappa and any user-defined response function
Chiou	Kinematic finite source: • Self-similar spatial distribution of slip • Scale-dependent rise time	• Complete Green's function for a layered crust.	• Model parameter	• Kappa
Hutchings/ Jarpe	• Kinematic rupture; parameters are geometry, hypocenter, rupture velocity, healing velocity (rise time), and roughness	• Inherent in selected empirical EUS Green's functions	• Inherent in selected empirical EUS Green's functions	• Inherent in selected empirical EUS Green's functions
O'Connell	• Finite with a semi-fractal slip velocity distribution • Variable rupture and healing velocities • Self-healing high-stress-drop asperities • Variable rise time and radiation pattern	• 1/R geometric spreading with isochrons	• Empirical WUS scattering functions	• Included in empirical WUS scattering functions
Papageorgiou	• Finite specific barriers; model of circular crack used to represent sub-events • Sub-event stress drop (local stress drop) • fmax	• Green's function	• Scattered wave energy (Zeng et al., 1991 or Sato, 1989 models)	• From variations of velocity in the upper km of crust
Silva	• Finite Brune sub-event • Finite slip distribution from f-k model • Constant rupture velocity, randomized rise time, rake, average radiation pattern	• Either 1/R geometrical spreading or • 1-D or 2-D ray trace	• Empirical EUS model	• Kappa/equivalent linear for nonlinear site-specific response
Somerville	• Finite with slip distribution from f-k model • Variable rake, rise time, radiation pattern • Low f: continuous slip function with theoretical radiation pattern • High f: discretized grid with empirical source functions, corrected to the source	• Low f: Green functions from f-k integration, complete response and Q for layered medium • High f: simplified Green functions from G-R theory, dominant rays and Q for layered medium • 2- and 3-D modeled with G-R for high f and finite difference for low f	• Empirical WUS model	• Inherent in selected empirical source functions, corrected for kappa

SECTION 3
MODEL VALIDATION AND ESTIMATION OF VARIABILITY

The essence of the validation process is calibrating any set of model parameters associated with a modeling method by limiting the misfit between the predicted and recorded motions. The residuals after optimization measure the inability of the method to predict the set of validation earthquake motions. In forward modeling exercises, following validation, the event-specific optimized parameters must be randomized to describe the range of parameter values that may occur in subsequent events.

The validation earthquake selected for the MCEER workshop is the 1988 Saguenay earthquake. It is the largest recorded ENA event and is documented by the most strong motion records of any ENA events. The exercise is to model the observed strong motions at nine stations on rock. Primarily, the validation is intended to assess to what extent each model predicts ground motions from a single previously recorded ENA earthquake. Because it also provides the participants the opportunity to calibrate individual model parameters, and insofar as these parameters are the basis for the subsequent scenario model estimates, the model calibrations enable each participant to provide the best possible estimates of ground motion.

Several of the models were previously validated against other earthquakes. These models should therefore be more finely tuned and capable of providing more robust ground motion estimates than those less well studied. Table 3-1 summarizes the number of validation earthquakes against which each model has been compared.

TABLE 3-1 Model Validation Summary

Modeler	Number of Earthquakes					Empirical Attenuation
	WUS	EUS	Subduction	Other	Total	
Anderson and Ni	5	1	0	3	9	No
Atkinson/Beresnev	1	1	2	0	4	Yes
Chiou	0	1	0	0	1	No
Hutchings and Jarpe	2	1	0	1	4	No
O'Connell	4	0	0	0	4	No
Silva	15	3	3	1	22	No
Somerville	6	4	4	0	14	No
Papageorgiou	6	2	0	0	8	No

Typically in validation studies, various source, path, or site parameters are prescribed that are based on results of independent studies of the validation earthquake. No such requirements were set forth in this study. Rather, the participants were allowed to calibrate any set of

parameters they deemed appropriate to the region and for the exercise. Discussion of model parameters was not a focus of the workshop.

3.1 Validation Earthquake

The scope of the workshop only allowed for a single validation earthquake. Two recent earthquakes were considered for use as the validation earthquake: the 1988 Saguenay, Ontario and the 1985 Nahanni, NW Territories events. The Saguenay event, an ENA earthquake, was well-recorded over a wide range of distances but its spectral content suggests that the mechanism may be anomalous compared to most other ENA and WUS earthquakes (see below). The Nahanni event has spectral content typical of ENA earthquakes but was recorded over an extremely limited distance range (about 8 to 16 km) and is not, technically, an ENA event. These limitations were judged to be significant enough that the Saguenay event was selected as the validation event.

The 25 November 1988 Saguenay earthquake was the largest to have occurred in ENA since the 1963 Baffin Bay event. The earthquake originated in the Grenville tectonic province of southern Quebec, in a relatively aseismic zone, with a nearly pure thrust mechanism (Somerville et al., 1990). The Saguenay event produced the largest set of strong motion records of any earthquake in the region: it was recorded at twelve sites within 200 km of the epicenter (Figure 3-1). Nine of the record sets from stations on rock sites were used in the validation studies (Table 3-2). Various magnitude estimates that describe the earthquake are (approximately): M_W 5.8, m_{bLg} 6.5, m_N 6.5 (short period magnitude), and m_b 5.9. The large discrepancy between m_{bLg}, m_N, and other scales was attributed to the spectral content of the source.

TABLE 3-2 Stations Used in Saguenay Validation Study

Station Number	Station Name	Distance (km)
S01	St-Ferreol	114
S02	Quebec	150
S05	Tadoussac	110
S08	La Malbaie	94
S09	St-Pascal	123
S10	Riviere-Ouelle	114
S16	Chicoutimi Nord	48
S17	St-Andre-du-Lac	66
S20	Les Eboulements	91

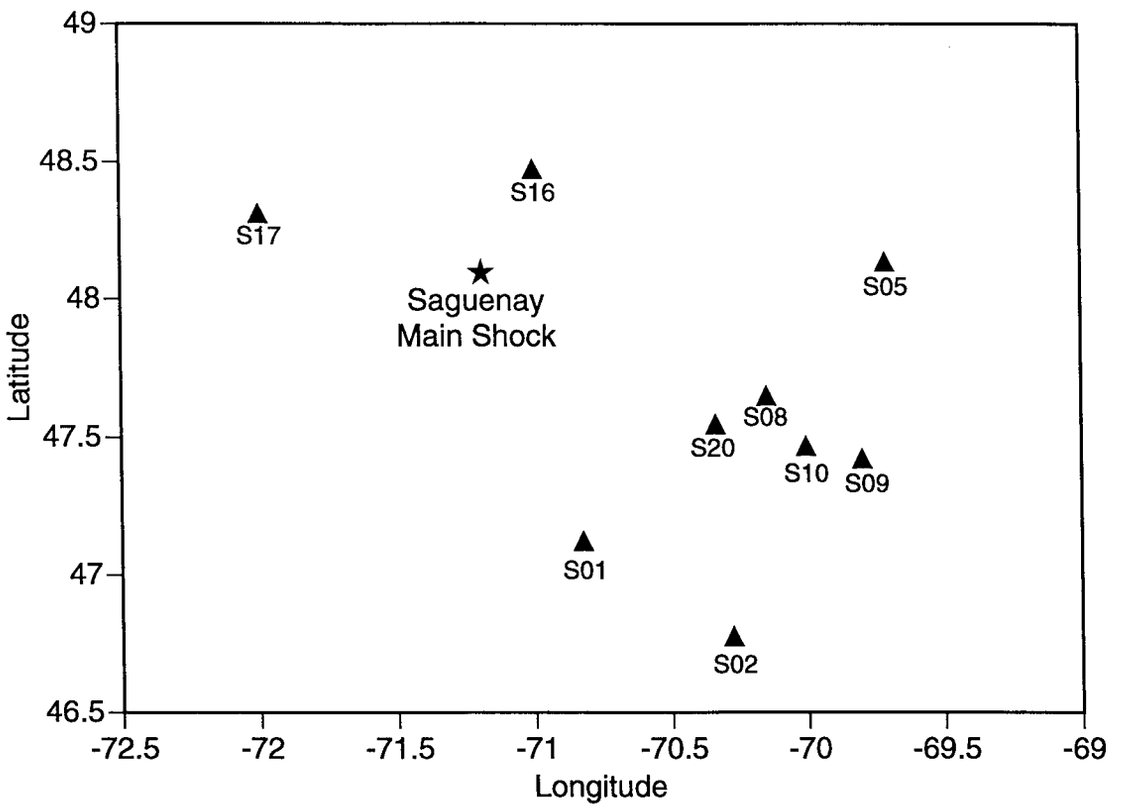

FIGURE 3-1 Saguenay Main Shock Epicenter and Strong Motion Recording Stations Used in Validation Exercises

This earthquake differed in two significant ways from other recent ENA events. Firstly, the focal depth, about 29 km, is notably deeper than most earthquakes in ENA which typically range from 5 to 15 km for larger events, causing critical reflections from the lower crust to occur at closer distances (Somerville et al., 1990). Only the 1968 Illinois event is known to have occurred at a similar depth. The centroid depth of about 26 km is based on an analysis of depth phases from teleseisms (Somerville et al., 1990) and is consistent with the deep hypocenter. Secondly, the high-frequency motion radiated from the source was exceptionally high and resulted in the over 0.5 magnitude unit difference between high frequency and other magnitude measures. The rich high-frequency content was not evident in other large earthquakes in the Saguenay sequence. Source studies have found that the main shock source was, in fact, not consistent with a single ω^{-2} source model (Boatwright and Choy, 1992). Haddon (1992) modeled the recorded motions with a unilateral rupture and short rise-times and concluded that these factors could account for the high-frequency content and Brune-scaling anomalies. However, Hartzell et al. (1994) derived a source model that consists mainly of a single compact asperity having a peak displacement of 2.6 m (high stress drop), which may account for the large ground motions. Lastly, ground motion levels significantly exceed those predicted using ENA attenuation relations within distances of about 120 km (Boore and Atkinson, 1992). This may be accounted for by the strong asperity, the large high-frequency energy radiated, unilateral rupture, or crustal characteristics resulting in a large "Moho bounce."

3.2 Results of Validation Exercise

The validation procedure involves optimizing any event-specific model and with the recorded ground motions. The validation process should include comparisons for a large number of earthquakes to evaluate the mean bias and modeling variability of the methods, however, for this exercise, we have only used one event to demonstrate the procedure. The strengths of the modeling methods should not be judges solely on the validation exercise from this one event.

In this study, the validation exercise using the Saguenay event was conducted for five of the models - Anderson/Ni, Atkinson/Beresnev (generic), Chiou, Hutchings and Silva. Somerville had validated his had validated his model previously (Somerville et al., 1990). Atkinson/Beresnev had also validated their stochasitc finite-fault model to the Saguenay earthquake as well as a WNA event and two subduction earthquakes (Beresnev and Atkinson, 1997, 1998b, 1998c). For the purposes of this study, they applied a generic ENA model and not one optimized for the Saguenay event. Both are generic and the optimized Saguenay validations for Atkinson/Beresnev are included.

Table 3-3: Summary of Realizations Performed in Saguenay Validation

Modeler	Number of Stations	Components			
		Horizontal H1	Horizontal H2	Average Horizontal	Vertical
Recorded Data	9	x	x		x
Anderson	9	x	x		x
Atkinson	9			x	
Chiou	9	x	x		x
Hutchings	9	x	x		x
Silva	9	x	x		

Recorded motions are compared to synthetics at all nine stations for the five models, in Appendix B. Included are seismograms (acceleration, velocity and displacement, horizontal and vertical), spectral acceleration (horizontal and vertical), and duration of motion (acceleration, velocity, and displacement; horizontal and vertical). Acceleration and velocity time histories for the two closest stations (16 and 17, at Chicoutimi Nord and St-Andre-du-Lac) are shown in Figures 3-2 and 3-3. Similar plots for two of the more distant stations (1 and 8, at St-Ferreol and La Malbaie) are shown in Figures 3-4 and 3-5. Most of the predictions give a reasonable agreement to the shape of the recorded time history during the strongest shaking, but the amplitudes can vary by a factor of 4 in peak ground acceleration (PGA). The response spectra of the predicted and recorded ground motions for these four stations are compared in Figure 3-6. At individual frequencies, the response spectra from the various model predictions vary by factors of 3 to 10.

The acceleration duration of the predicted and recorded ground motions for the four stations are compared in Figure 3-7. The duration is defined using the normalized Arias intensity. The duration is the time interval between 5% and 100x% of the arias intensity. For example, the time interval between 5% and 90% of the arias intensity is plotted at x=0.9. Similarly, the time interval between the 5% and 50% arias intensity is plotted at x=0.50. These plots indicate how the energy is distributed through time in the ground motion. The alternative simulation procedures vary in duration by a factor of 5 to 10.

The horizontal spectral acceleration residuals for the nine Saguenay stations are shown on the left hand side of Figure 3-8 for the individual simulation models. The standard deviation of the residuals is shown on the left hand site of this figure. The average residual computed from all nine Saguenay stations for the models are compared in the top frame of Figure 3-9a. The lower frame compares the standard deviation of the residuals. There is no consistent trend of over- or under-prediction with frequency for all of the models. Overall, the Anderson/Ni model shows the least bias at all periods. The modeling variability similarly shows no single trend with period; they are generally between about 0.6 and 1.0 natural log units.

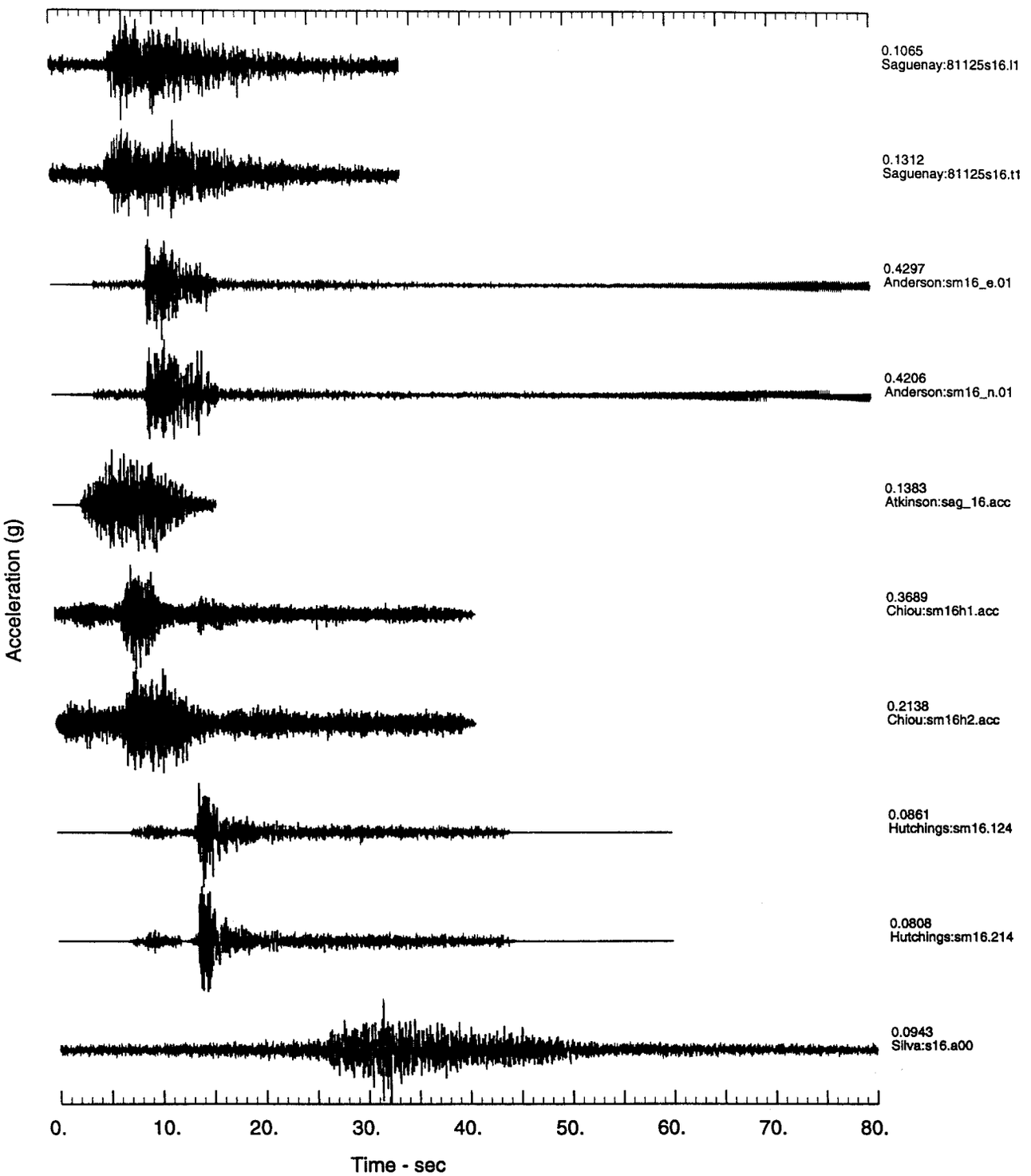

FIGURE 3-2a Comparisons of Recorded Chicoutimi Nord Accelerations and Validation Synthetics, Horizontal Components

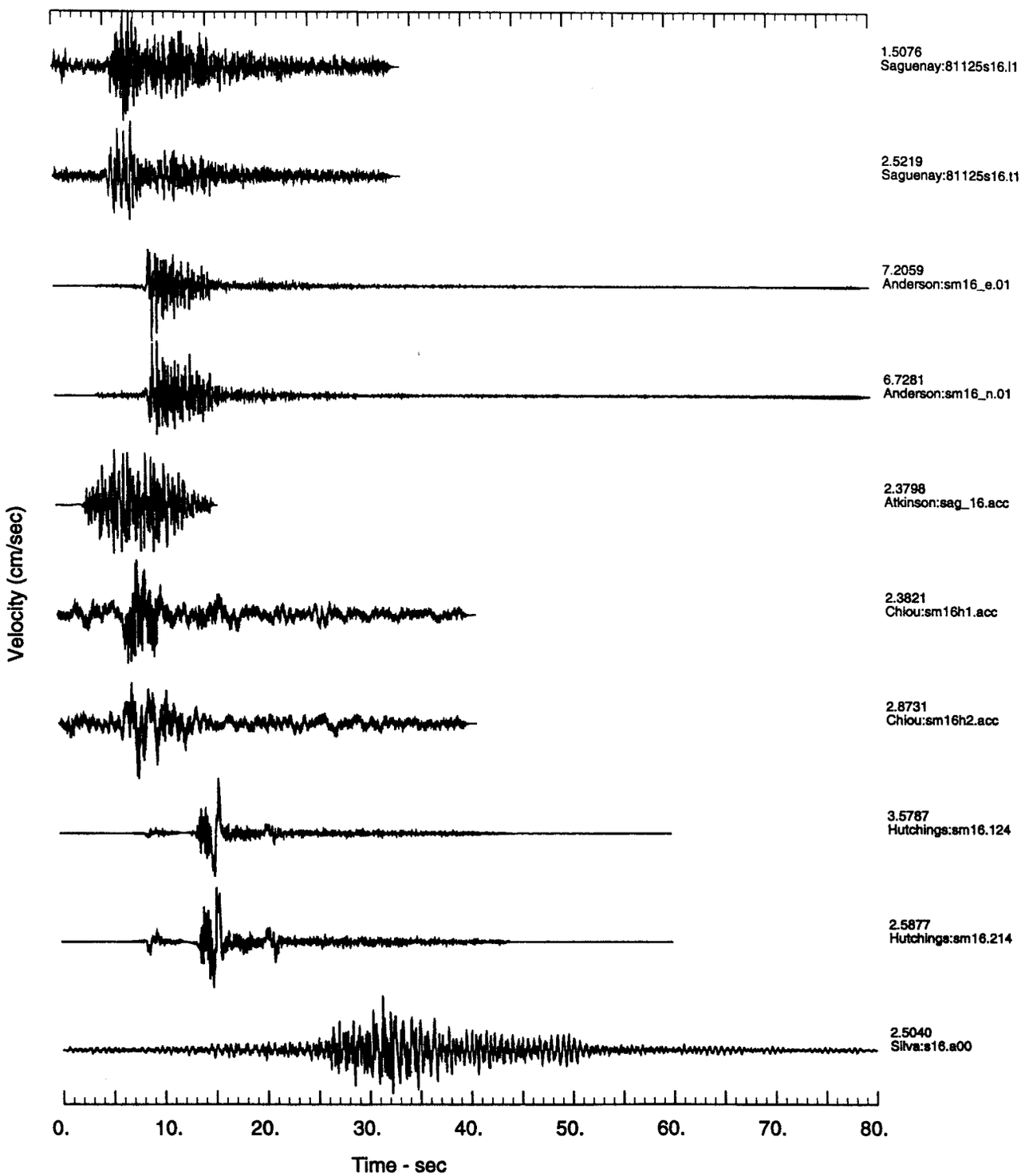

FIGURE 3-2b Saguenay Validations, Horizontal Velocity Components: Chicoutimi Nord

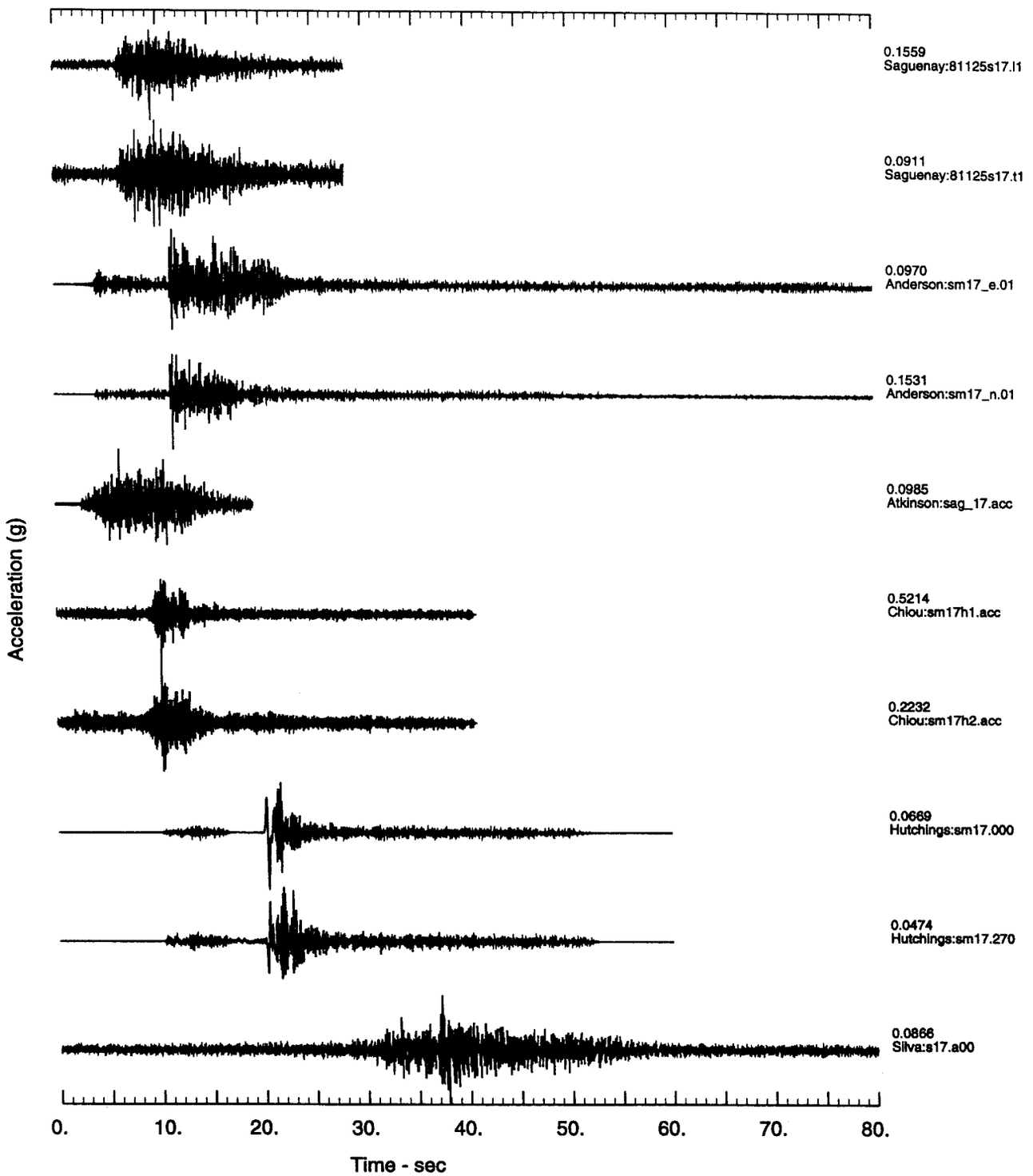

FIGURE 3-3a Comparisons of Recorded St-Andre-Du-Lac Accelerations and Validation Synthetics, Horizontal Components

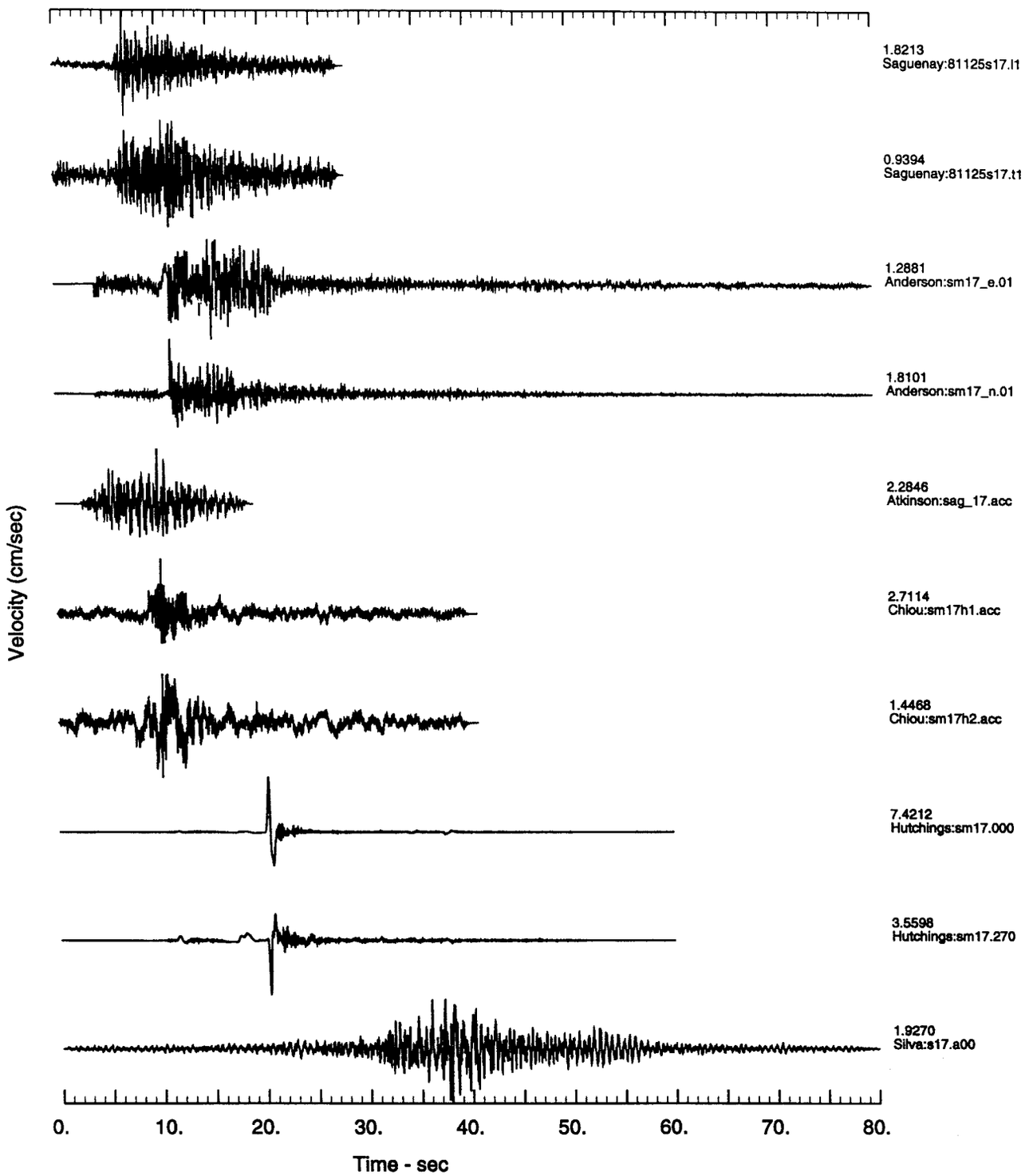

FIGURE 3-3b Saguenay Validations, Horizontal Velocity Components: St-Andre-Du-Lac

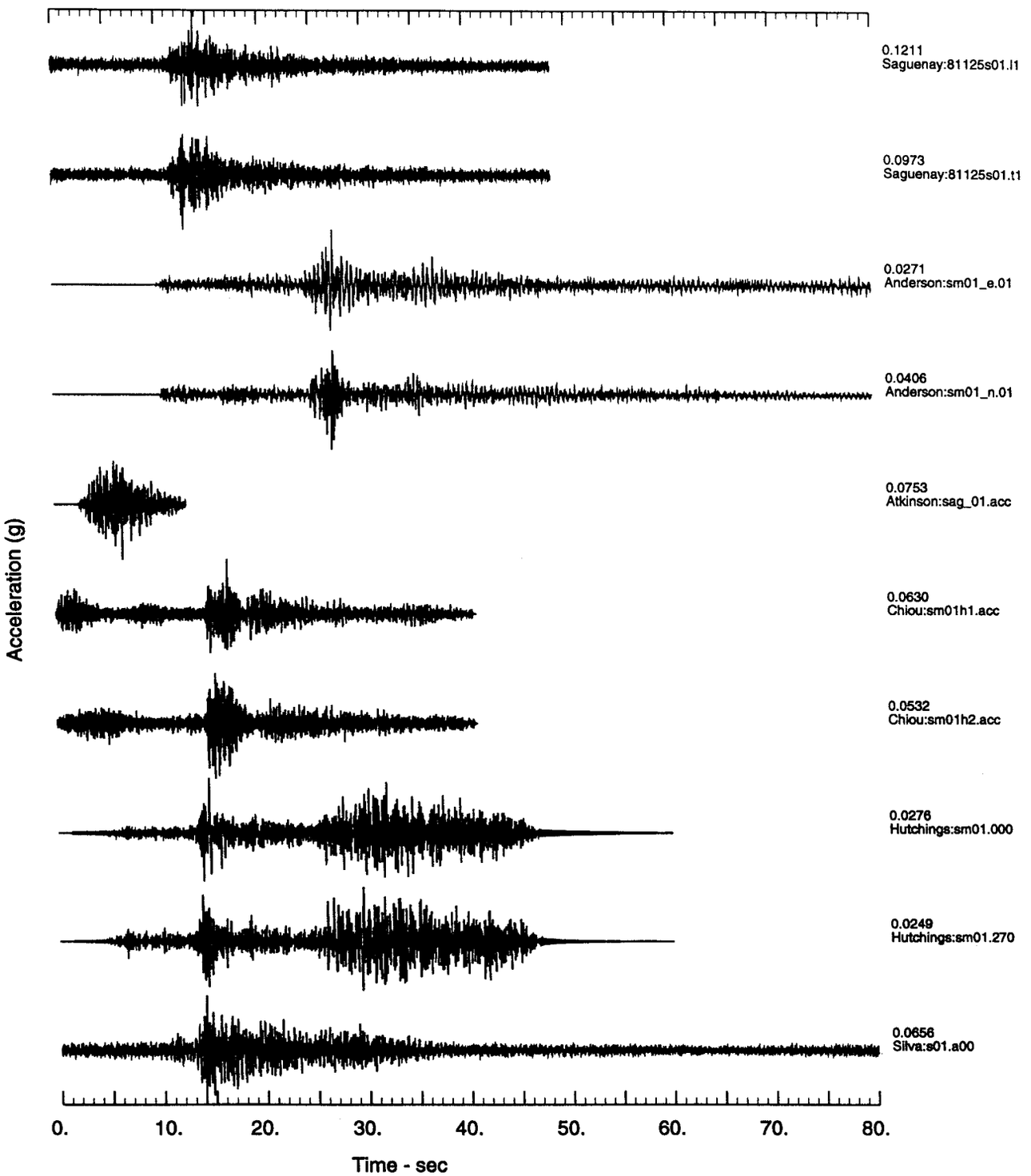

FIGURE 3-4a Comparisons of Recorded St-Ferreol Accelerations and Validation Synthetics, Horizontal Components

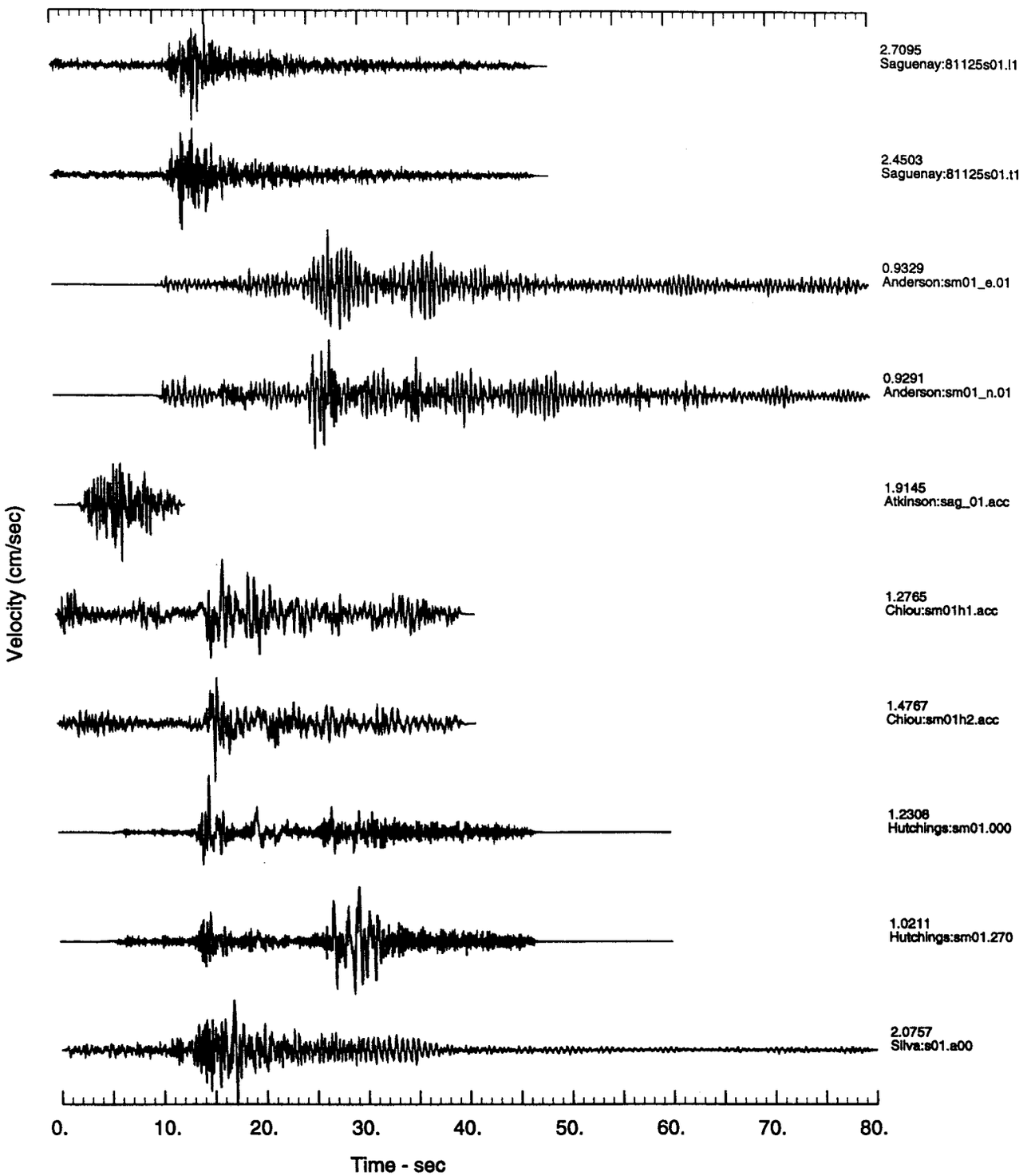

FIGURE 3-4b Saguenay Validations, Horizontal Velocity Components: St-Ferreol

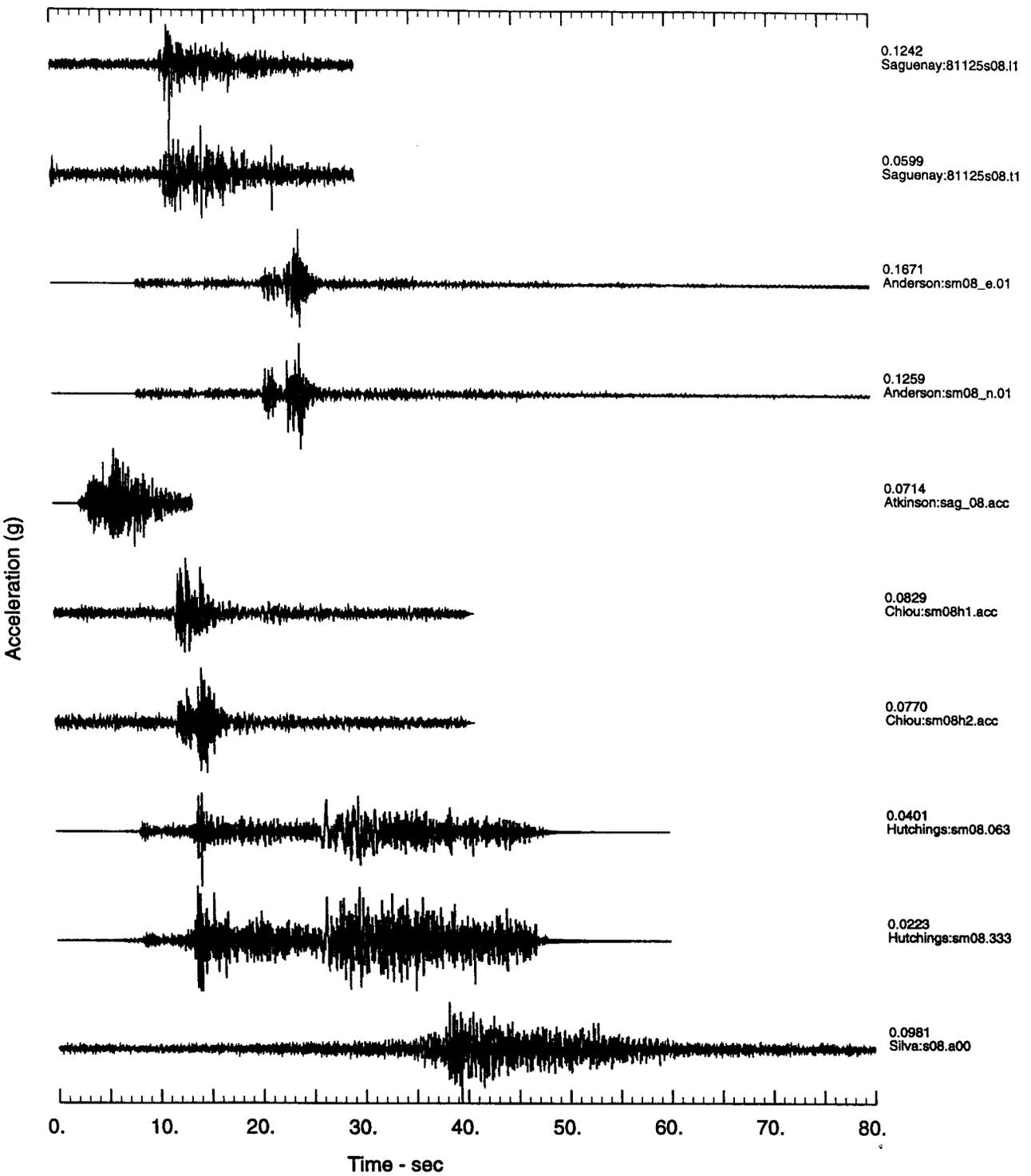

FIGURE 3-5a Comparisons of Recorded La Malbaie Accelerations and Validation Synthetics, Horizontal Components

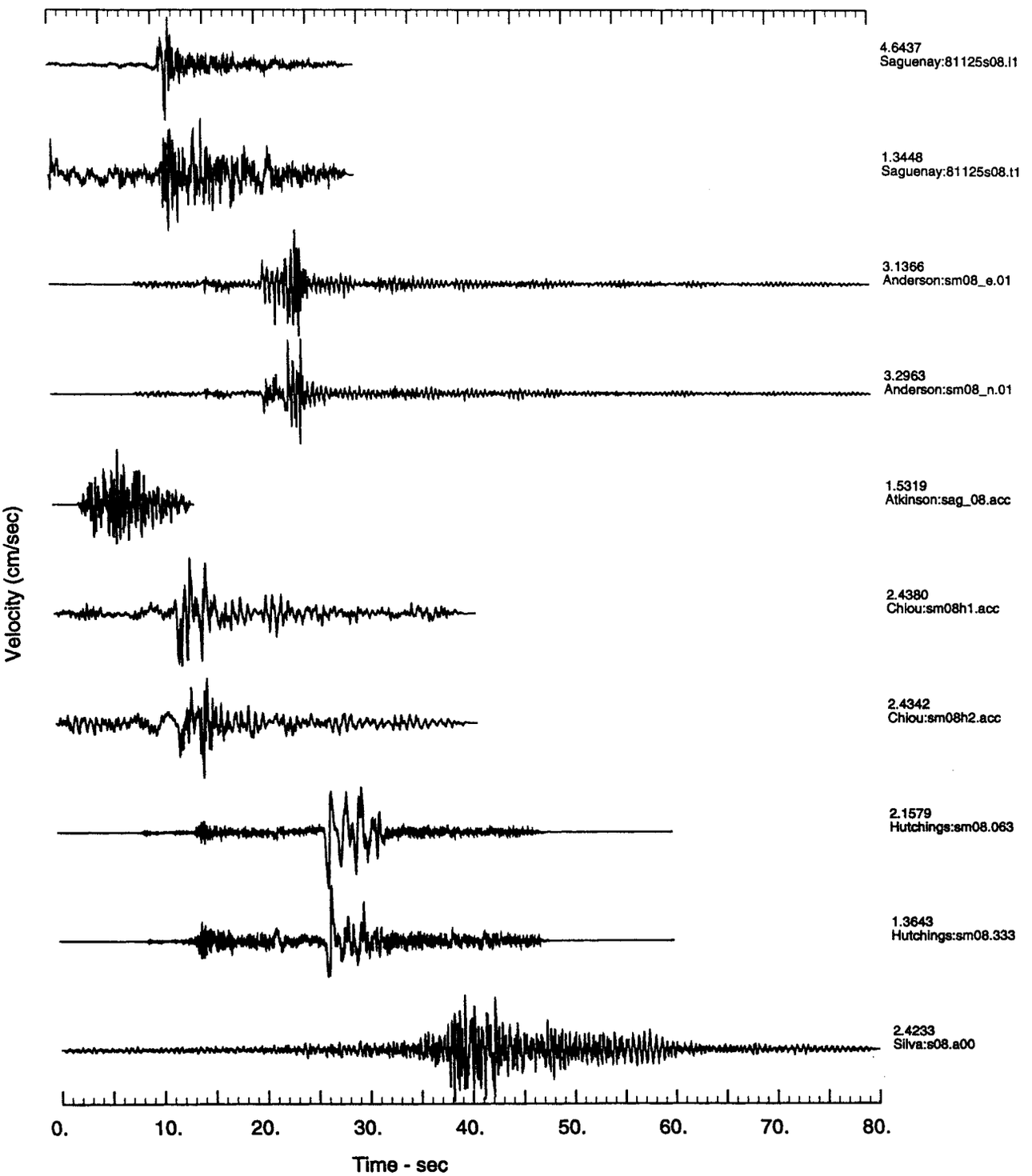

FIGURE 3-5b Saguenay Validations, Horizontal Velocity Components: La Malbaie

The mean residual and modeling variability shown in Figure 3-9a is for only one earthquake. This is not an adequate data set on which to develop robust model bias and modeling variability estimates. Some of the simulation methods had been previously validated against a larger number of earthquakes. Anderson/Ni, Silva, Somerville, and Atkinson/Beresnev each have previously computed model bias using several EUS and WUS earthquakes. The model bias and modeling variability for these more extensive validations are shown in Figure 3-9b. For these more extensive validations, the model bias and modeling variability are much smaller at high frequencies than for the Saguenay validation by itself.

The residuals for acceleration duration for the Saguenay validation are shown in Figure 3-10. The Anderson/Ni model shows the least bias over all intensity intervals. The Atkinson/Beresnev model tends to underpredict the acceleration duration whereas the Chiou, Hutchings and Silva models tend to overpredict the acceleration duration.

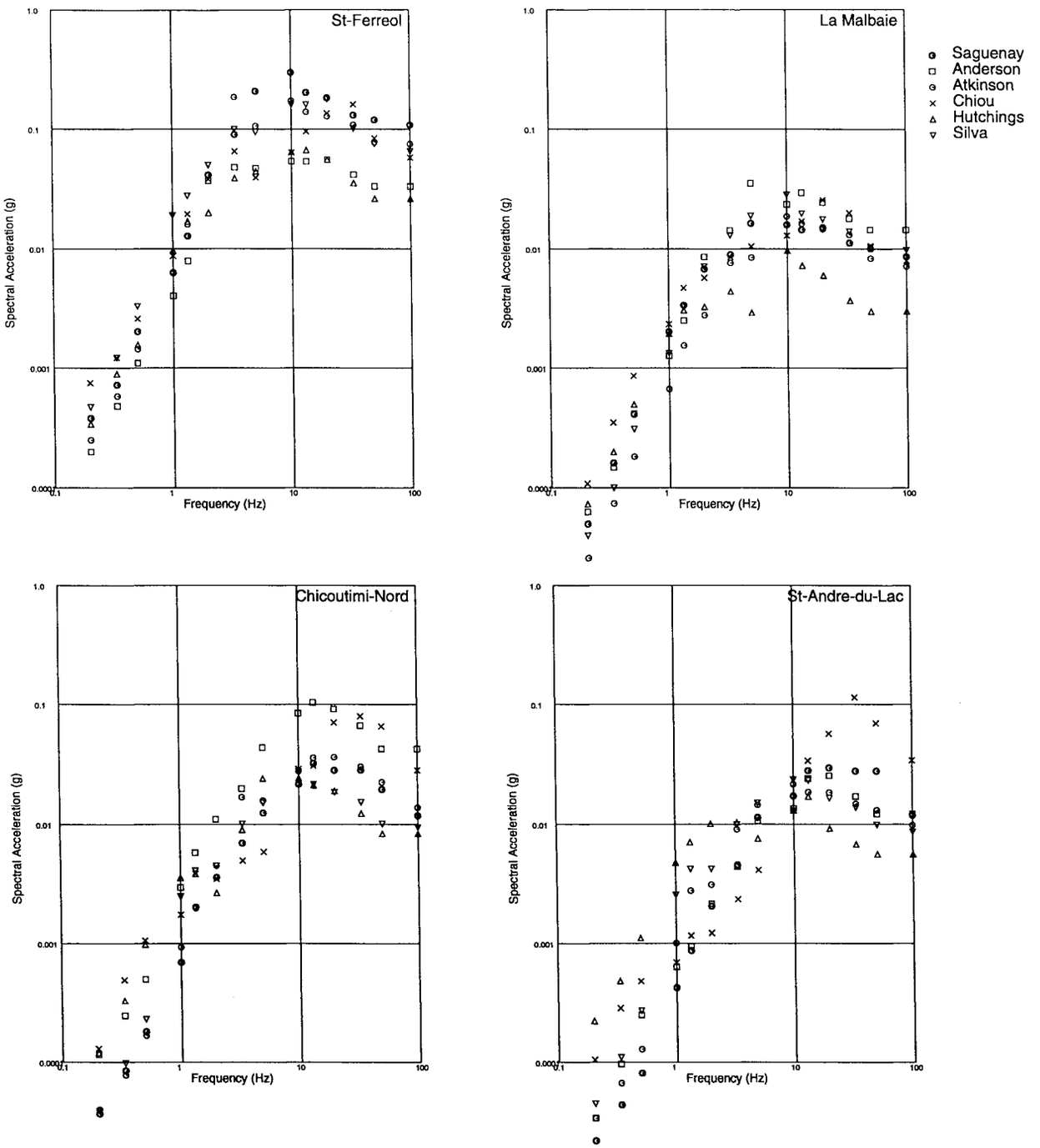

FIGURE 3-6 Spectra Comparisons for Saguenay Recordings and Validation Synthetics, Horizontal Component, 5% Damping

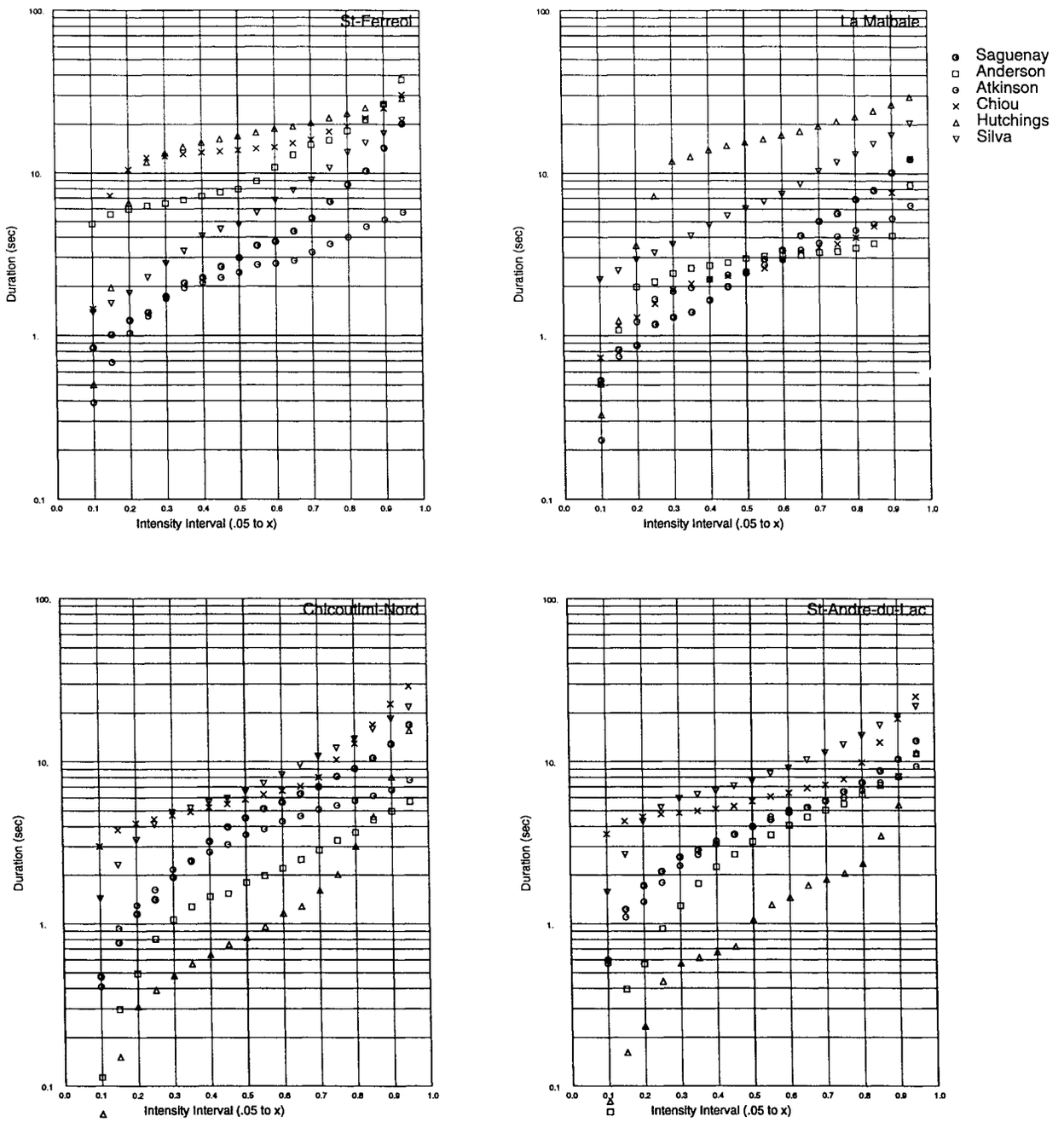

FIGURE 3-7 Comparison of Acceleration Durations Computed for Saguenay Records and Validation Synthetics, Horizontal Component

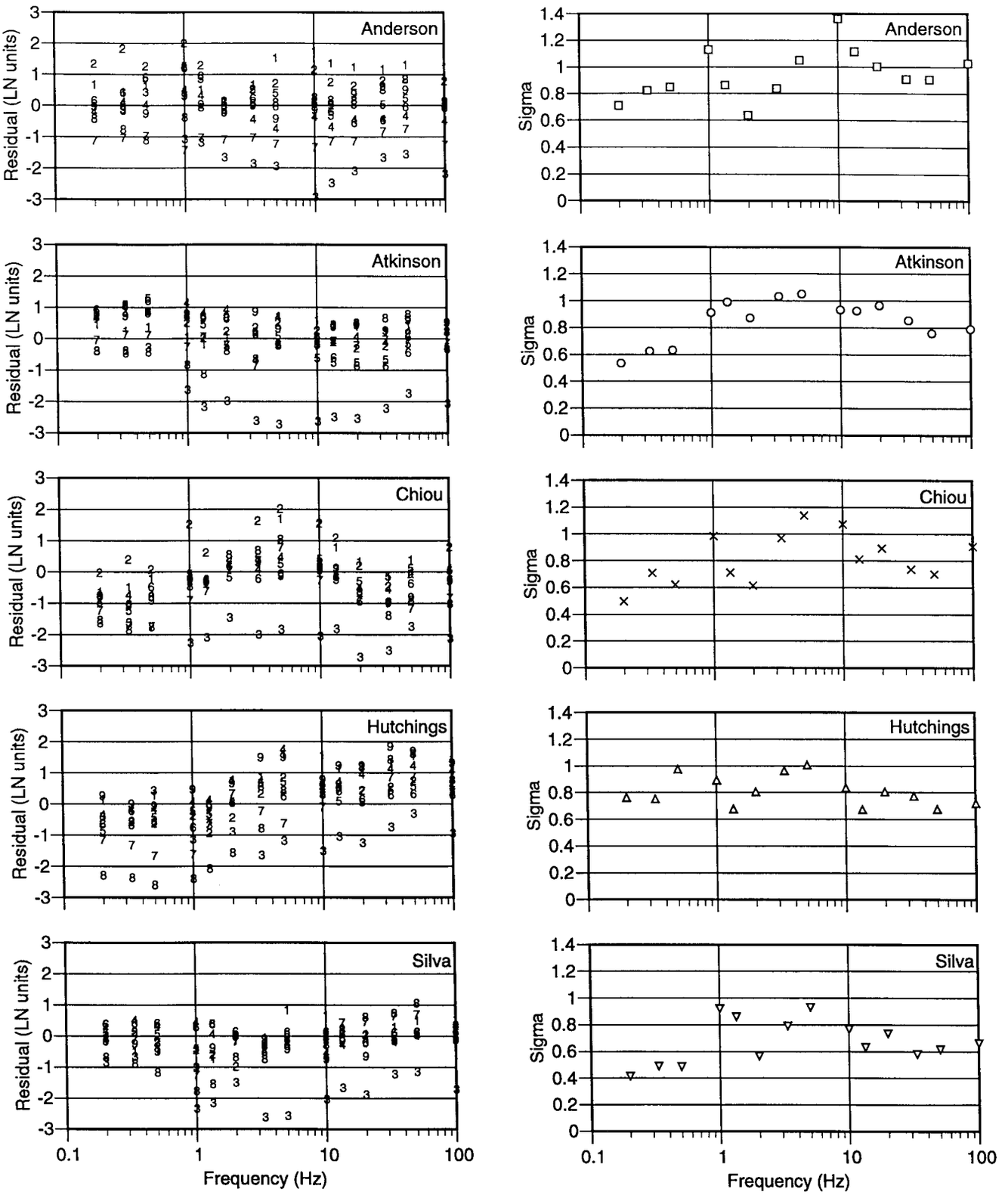

FIGURE 3-8 Residuals of Horizontal Spectral Acceleration for the Nine Saguenay Stations

(Note: A positive model bias reflects underprediction, negative reflects overprediction. Residuals at each recording site are indicated by the order listed in Table 3-2.)

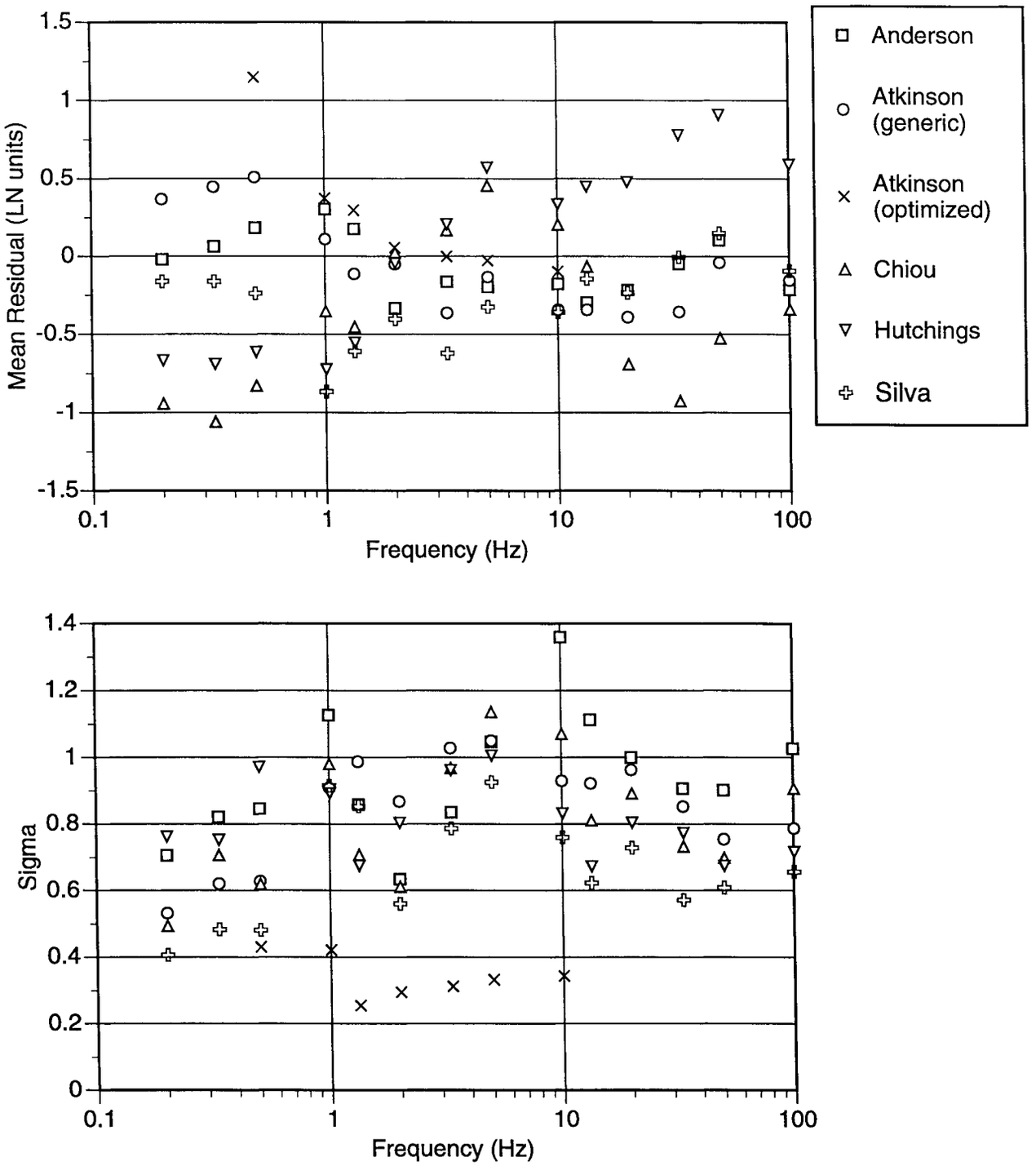

FIGURE 3-9a Model Bias and Modeling Variability Based on the Saguenay Earthquake Only (Average Horizontal Acceleration)
(Note: A positive model bias reflects underprediction, negative reflects overprediction.)

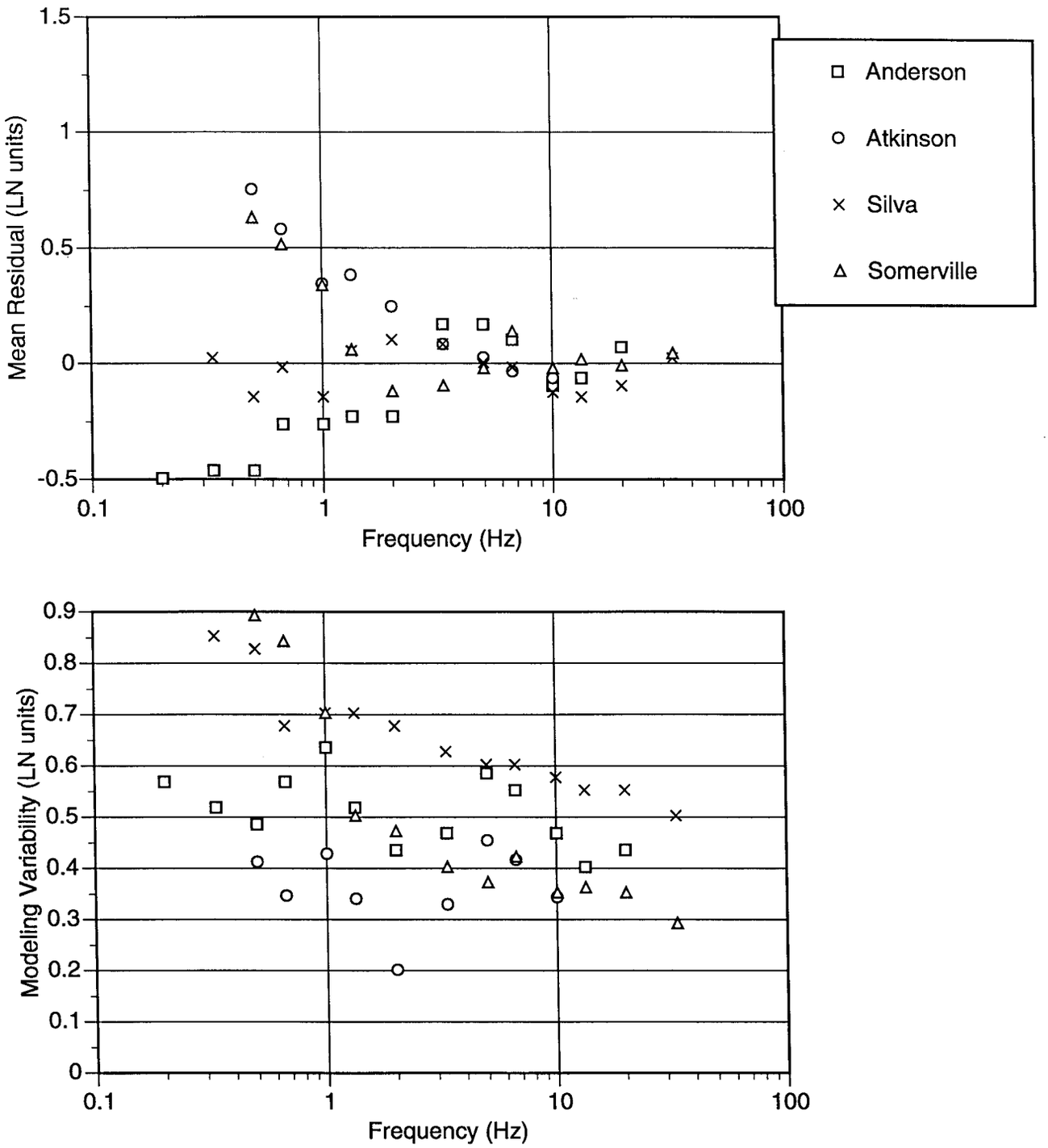

FIGURE 3-9b Model Bias and Modeling Variability Based on Various Other Validation Studies

(Note: A positive model bias reflects underprediction, negative reflects overprediction.)

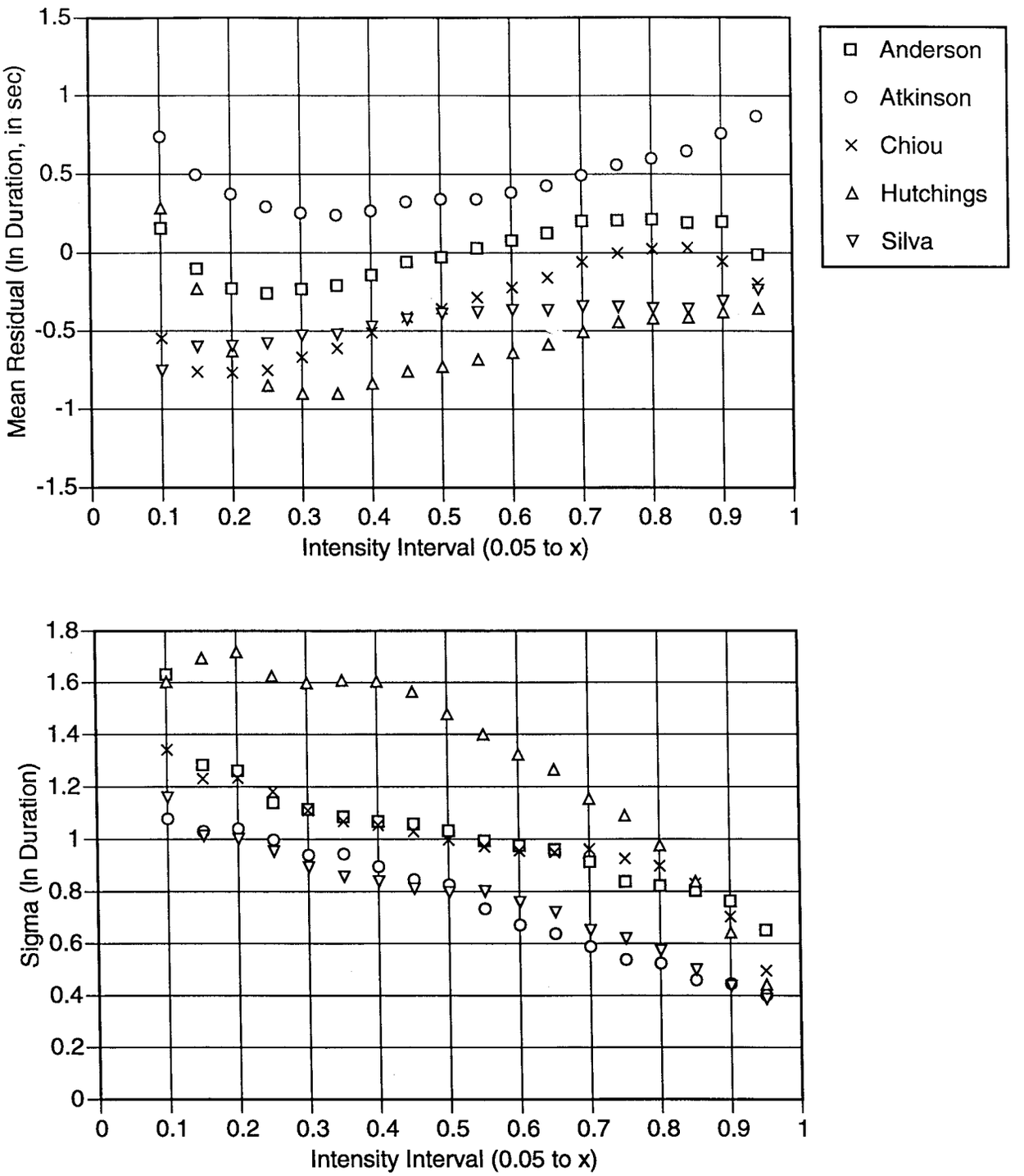

FIGURE 3-10 Model Bias and Modeling Variability Based on the Saguenay Earthquake Only (Horizontal Acceleration Duration)
(Note: A positive model bias reflects underprediction, negative reflects overprediction.)

SECTION 4
SCENARIO EVENT GROUND MOTIONS

In forward modeling of a scenario event, a fault geometry and select source, path, and site parameters are typically specified. Parameters not specified, including details of the rupture process and parameters optimized in the validation, are randomized to model the range of their uncertainty in future events.

In this study, fault geometry, event magnitude, event rake, velocity structure, and site kappa were all specified (Table 4-1). The scenario earthquake adopted for this study is a thrust event with moment magnitude 7.0 occurring on a 45° east-dipping plane. The fault dimensions are 50 km long and 20 km wide. The top of the rupture zone lies 2 km below the ground surface thus precluding energy release in the very near-surface. The EPRI Mid-continent crustal velocity model (Fig. 4-1) and Q-model were stipulated. Simulations were performed at a suite of 30 sites surrounding a dipping fault plane (Table 4-2, Fig. 4-2). All sites are hard rock.

Table 4-1a: Scenario Event Source Parameters

Magnitude	7.0
Event Rake	90°
Fault Dip	45°
Site Kappa	0.006
Q	$670 f^{0.33}$

Table 4-1b: EPRI Mid-Continent Crustal Model

Layer Thickness (km)	Depth to Layer Top (km)	V_P (km/sec)	V_S (km/sec)	Density (gm/cc)
1	0	4.9	2.83	2.52
11	1	6.1	3.52	2.71
28	12	6.5	3.75	2.78
-	40	8.0	4.62	3.35

The approaches adopted to represent source, path, and site effects are summarized in Table 4-3 for each participant. Each of the source parameters that were optimized in the validation exercise was to be varied in the simulations. These may have included slip model, hypocentral location, sub-event parameters, or any other parameters relevant to a specific model. Parameters that were randomized in the simulations by each participant are summarized in Table 4-4. A minimum of ten source realizations was suggested to define the parametric variability. Not all participants were able to provide a complete suite of synthetic motions, or

provide synthetics at each of the 30 sites. Motions that were provided are summarized in Table 4-5.

The output for the modeling exercise was standardized in order to facilitate comparisons of results. All ground motion estimates were provided as accelerations in g in a specified format. Three components of motion were requested, as appropriate for each model.

Table 4-2: Site Coordinates

Site	x-Dist (km)	y-Dist (km)
1	-10	5
2	5	5
3	10	5
4	25	5
5	50	5
6	80	5
7	100	5
8	120	5
9	150	5
10	200	5
11	300	5
12	500	5
13	-10	15
14	5	15
15	10	15
16	25	15
17	50	15
18	80	15
19	100	15
20	120	15
21	150	15
22	200	15
23	300	15
24	500	15
25	5	25
26	5	40
27	5	80
28	5	100
29	5	120
30	5	150

Table 4-3: Models for Source, Path, Scatterer and Site used in Scenario Realizations

Participant	Source	EUS[1] Source	Path	Scatterer	Site
Anderson/Ni	ω^2	$\Delta\sigma_{sub}$, $V_{rupture}$, R_{max}	FK, Q	Model	Q, kappa
Atkinson/ Beresnev	ω^2	RS^2 Factor, Sub-fault Size[3]	Empirical EUS	Empirical Duration	kappa
Chiou	ω^2	Rise Time	FK, Q	Model	kappa
O'Connell	Finite Fault	Variable local stress drop, rise times, and asperity positions	Rays	Empirical WUS[4]	Empirical WUS
Silva	ω^2		Rays, Q	Empirical EUS	kappa
Somerville	Finite Fault	Static $\Delta\sigma$	Green's Functions, Q	Empirical WUS	kappa
Hutchings/ Jarpe[5]	Kinematic		EUS Green's Function	EUS Green's Function	EUS Green's Function
Papageorgiou[5]	Circular Crack (Sub-event)	$\Delta\sigma_{Local}$ $\Delta\sigma_{Global}$	Green's Function	Scattered Wave Energy Model	Q (≈kappa)

Notes:

1 *Eastern U.S.*

2 *Fixed to Saguenay values*

3 *Radiation-strength factor*

4 *Western U.S.*

5 *Participant did not provide scenario motions; parameters shown reflect the model approach that would have been adopted*

Table 4-4: Parameters Randomized in Scenario Realizations

Participant	Randomized Parameters			Fixed Parameters[1]
	Hypocenter	Slip Distribution	Rise Time	
Anderson	x	x	x	$\Delta\sigma_{sub}$, R_{max} , $V_{rupture}$
Silva	x	x	x (Sub-event)	$\Delta\sigma_{sub}$, Mainshock Rise Time
Chiou	x	x	x	
Somerville	x	x	x	
Atkinson	x	x		RS Factor, Grid size
O'Connell	x	x	x	
Hutchings[2]	x	x	x	
Papageorgiou[2]	x	x		

Notes:

[1] *Parameters optimized in validation study*

[2] *Participant did not provide scenario motions; parameters shown are model approach that would have been adopted*

Table 4-5: Summary of Simulations Provided by Participants

Participant	Number of Stations[1]	Components Simulated				Number of Realizations Computed
		East	North	Average Horizontal	Vertical	
Anderson	26[2]	x	x		x	10
Atkinson	30			x		10
Chiou	25[3]	x	x		x	12
O'Connell	10[4]	x	x		x	800[5]
Silva	30			x		30
Somerville	26[6]	x	x		x	27

Notes:

[1] *30 possible*

[2] *Stations 11, 12, 23, and 24 were omitted.*

[3] *Stations 11, 12, 23, 24, and 30 were omitted.*

[4] *Stations modeled include 1, 2, 3, 4, 13, 14, 15, 16, 25, and 26.*

[5] *Ten slip models and the 1st, 21st, and 80th hypocenters generated by O'Connell were used (30 total).*

[6] *Stations 11, 12, 23, and 24 were omitted.*

4.1 Modeling Results

Each participant developed suites of synthetics at each of thirty sites surrounding the scenario rupture. All synthetics are shown in Appendices C through G for the six participants in the simulation exercise. Appendices H and I summarize the horizontal and vertical results as spectra and acceleration, velocity, and displacement duration. A sample of these results is reproduced as Fig. 4-3 through 4-20 at sites 1, 21, and 29. These are located on the footwall near the center of the rupture plane, 120 km normal to the strike of the plane on the hanging wall, and 150 km along-strike, respectively (Fig. 4-2).

The mean horizontal acceleration response spectra from the simulations are shown in Figures 4-3, 4-4, and 4-5 for the three sites. The horizontal spectra are all within a factor of 3-5 of each other for the close in site and the distant sites. The parametric variability is computed from each participants suite of realizations and is shown in the lower frame of Figures 4-3 to 4-5. The parametric variability is relatively small and ranges between about 0.1 to 0.4 (natural log units) at high frequencies and is slightly greater at low frequencies. This parametric variability is much smaller than the variability between mean model predictions.

The mean horizontal acceleration duration from the simulations is shown in Figures 4-6, 4-7, and 4-8 for the three sites. For the short distance site, four of the models produce similar durations: Anderson/Ni, Atkinson/Beresnev, Somerville, and Chiou. The Silva model produces much longer durations and the O'Connell model produces much shorter durations. For the two distant sites, the mean durations vary by about a factor of 2. The Anderson/Ni model, which includes scattering effects, produces the longest durations (Fig. 4-8). The parametric variability of the duration is shown in lower frame of Figures 4-6 to 4-8. For site 21, the parametric variability is very small (less than 0.2 natural log units) but for site 29, off the end of the fault, the parametric variability is much larger (0.1 to 0.6 natural log units). This increase in parametric variability is probably due to variable hypocenter locations leading to forward and backward directivity conditions.

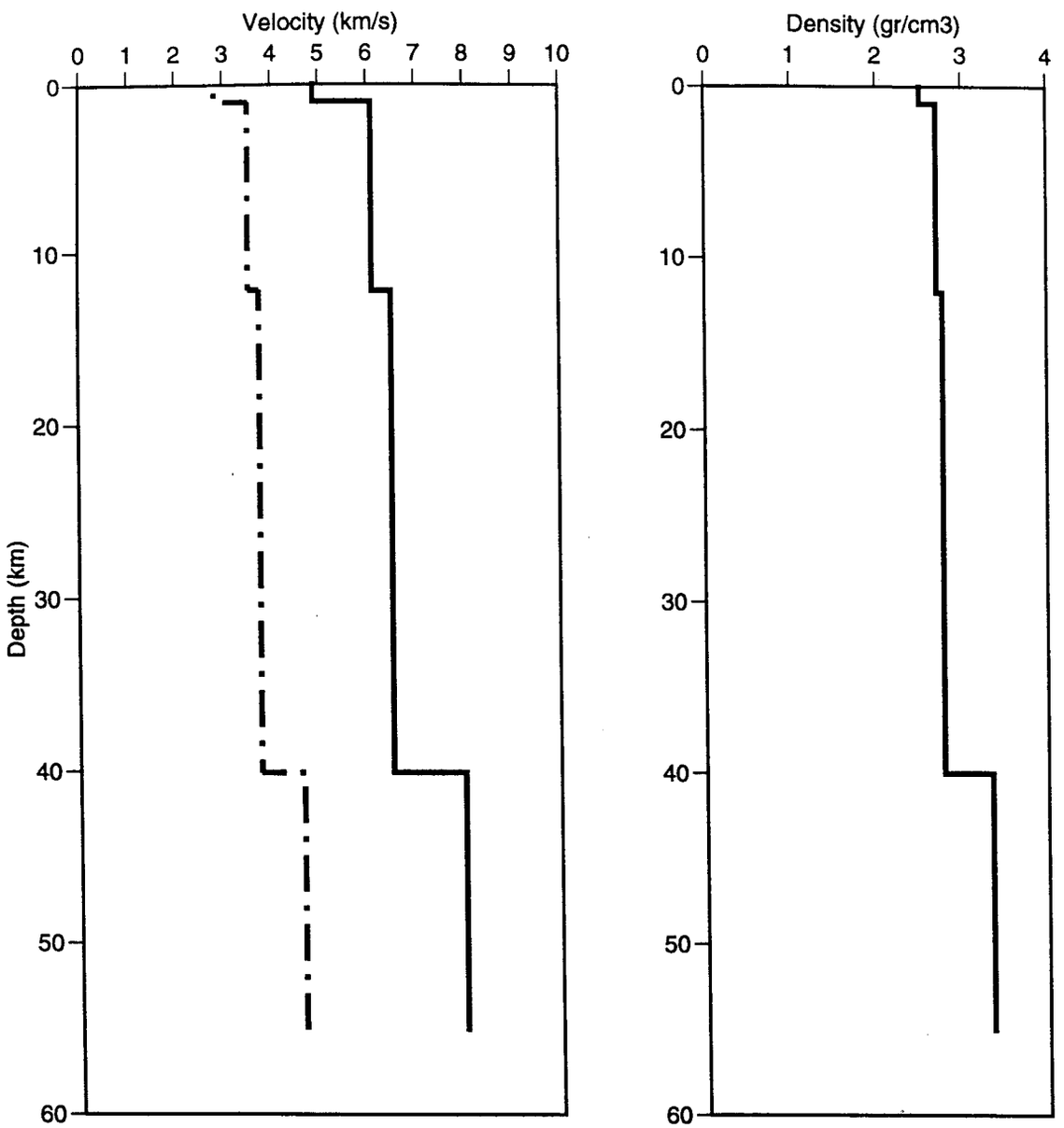

FIGURE 4-1 EPRI Mid-Continent Crustal Model

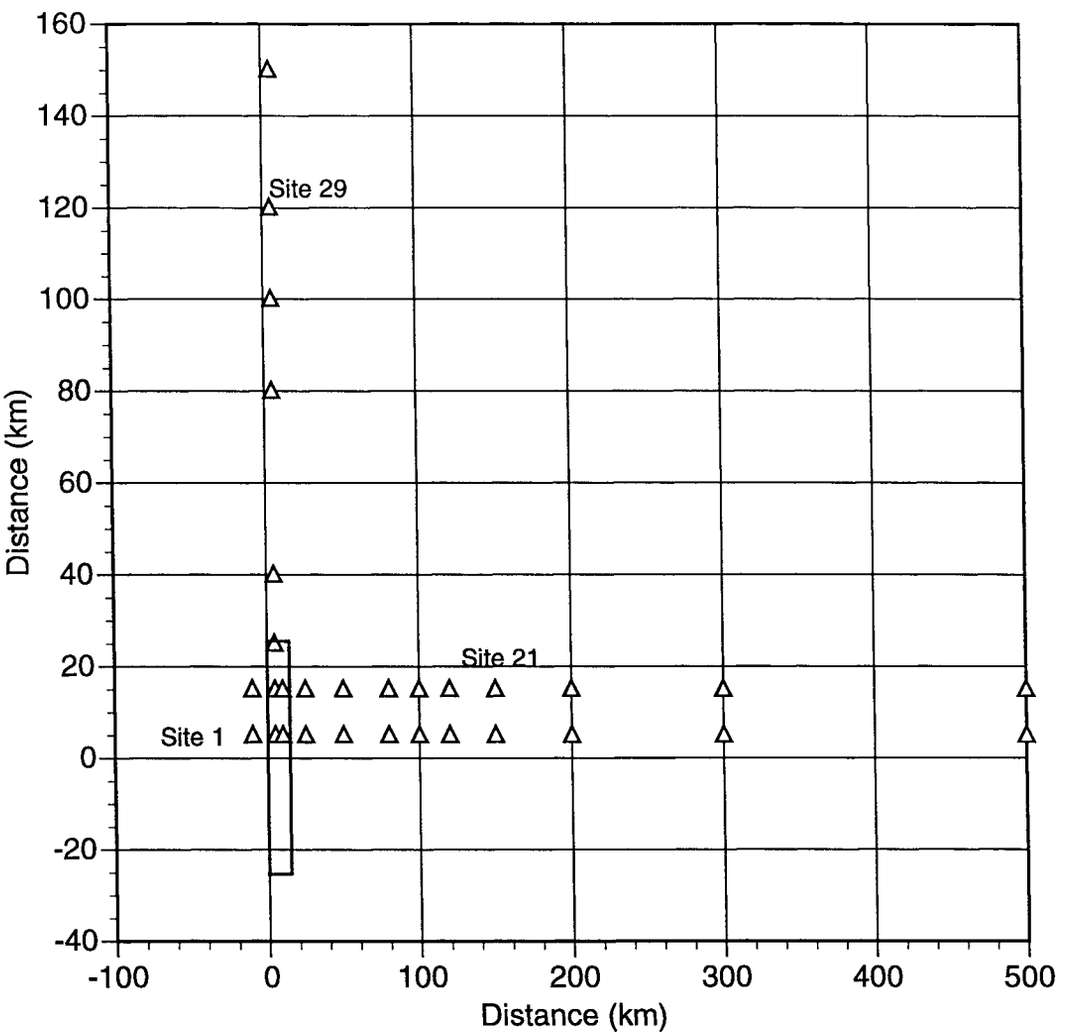

FIGURE 4-2 Simulation Exercise Fault Geometry and Site Locations

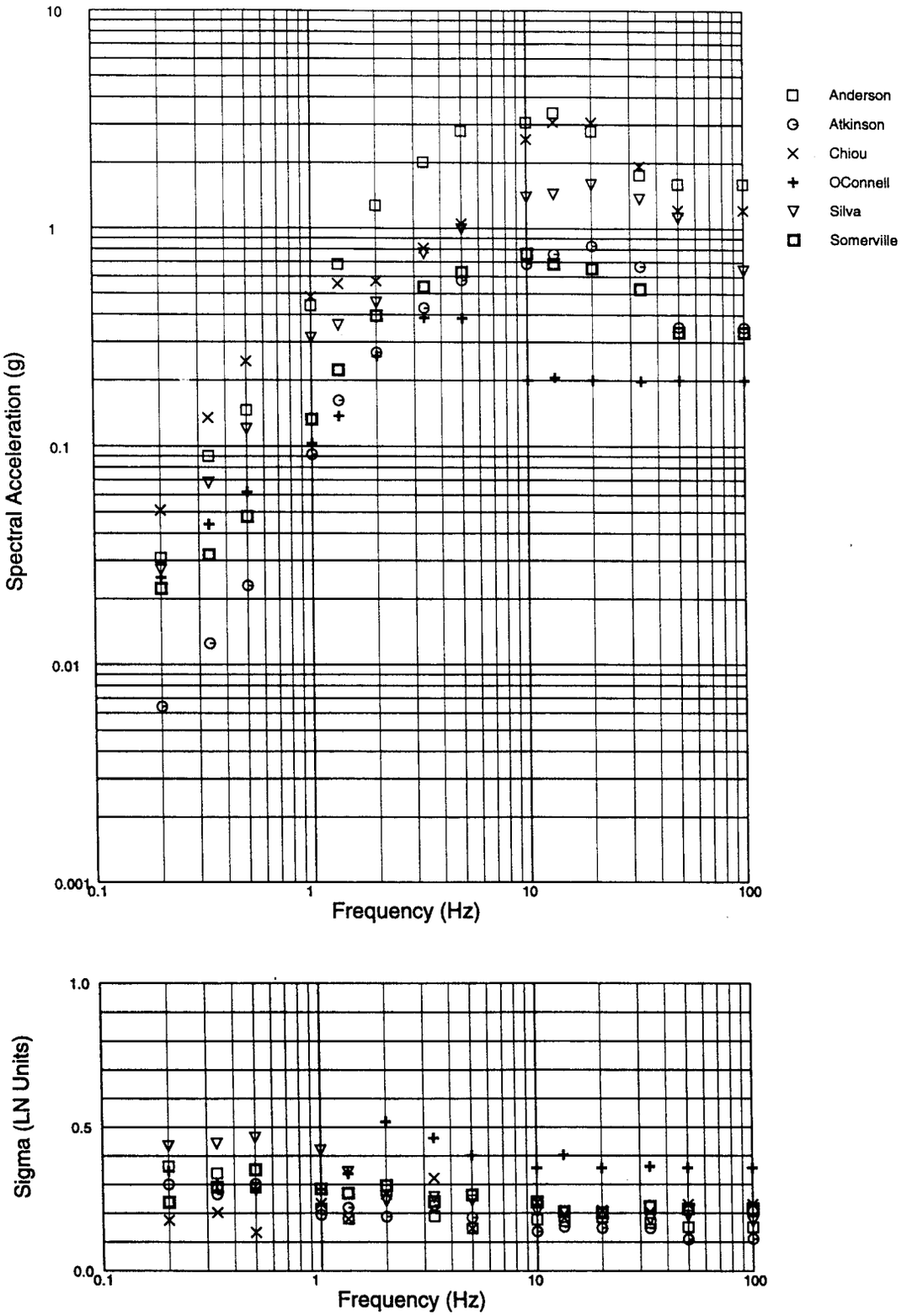

FIGURE 4-3 Scenario Site 1: Spectral Acceleration (5% Damping) and Parametric Variability of Horizontal Ground Motions Computed in Scenario Modeling Exercise (Note: The average spectrum of the two horizontal components is shown.)

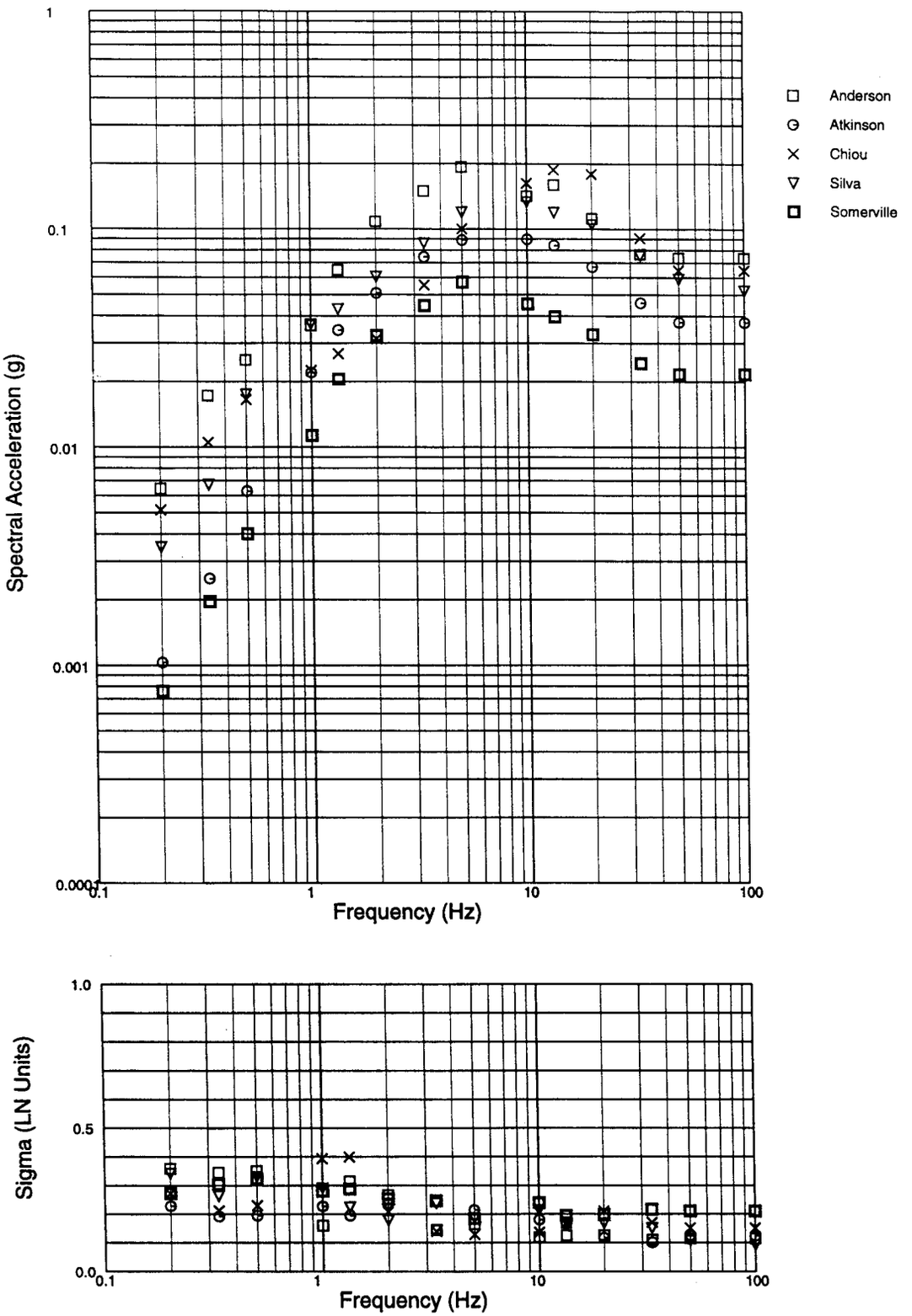

FIGURE 4-4 Scenario Site 21: Spectral Acceleration (5% Damping) and Parametric Variability of Horizontal Ground Motions Computed in Scenario Modeling Exercise (Note: The average spectrum of the two horizontal components is shown.)

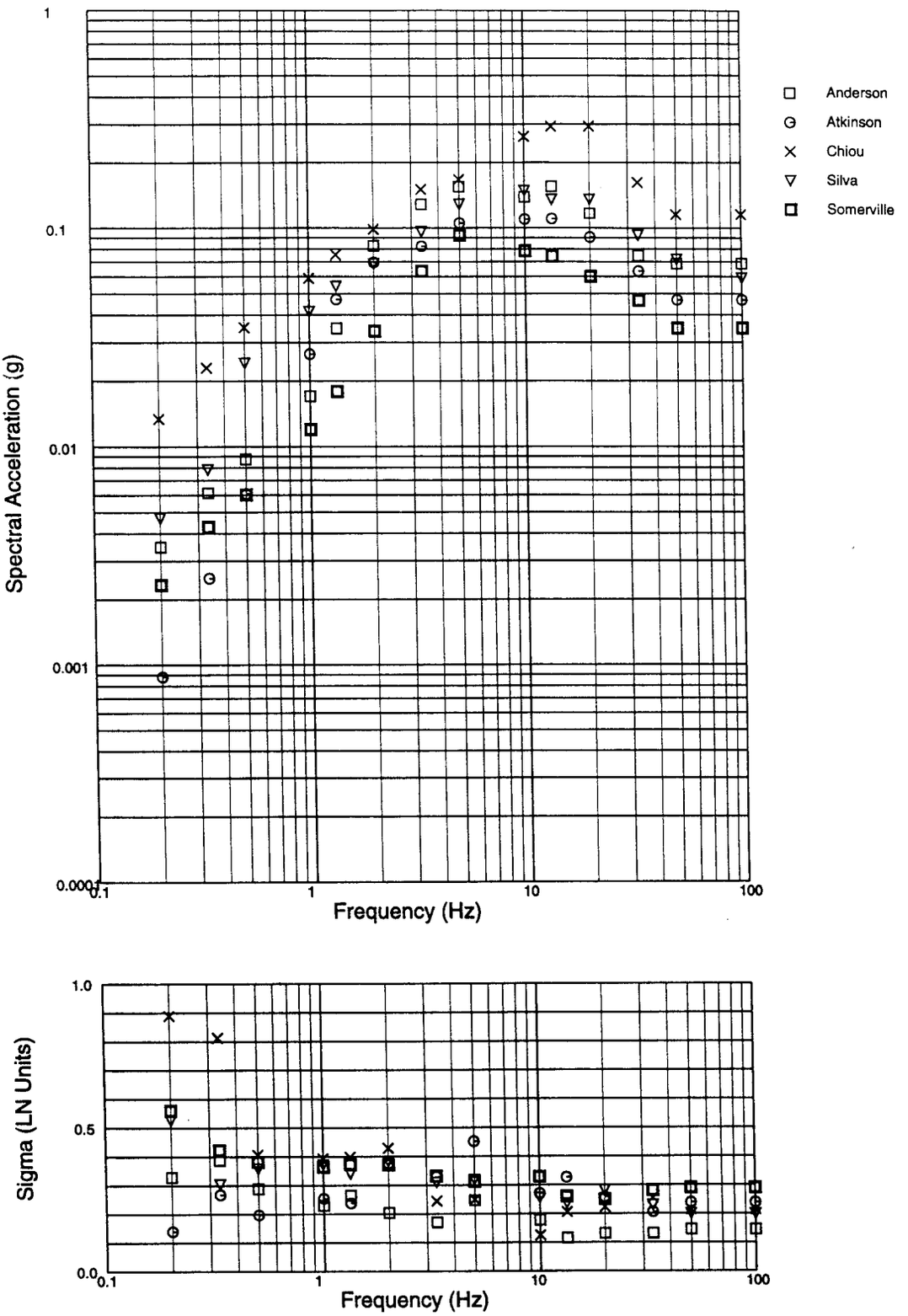

FIGURE 4-5 Scenario Site 29: Spectral Acceleration (5% Damping) and Parametric Variability of Horizontal Ground Motions Computed in Scenario Modeling Exercise (Note: The average spectrum of the two horizontal components is shown.)

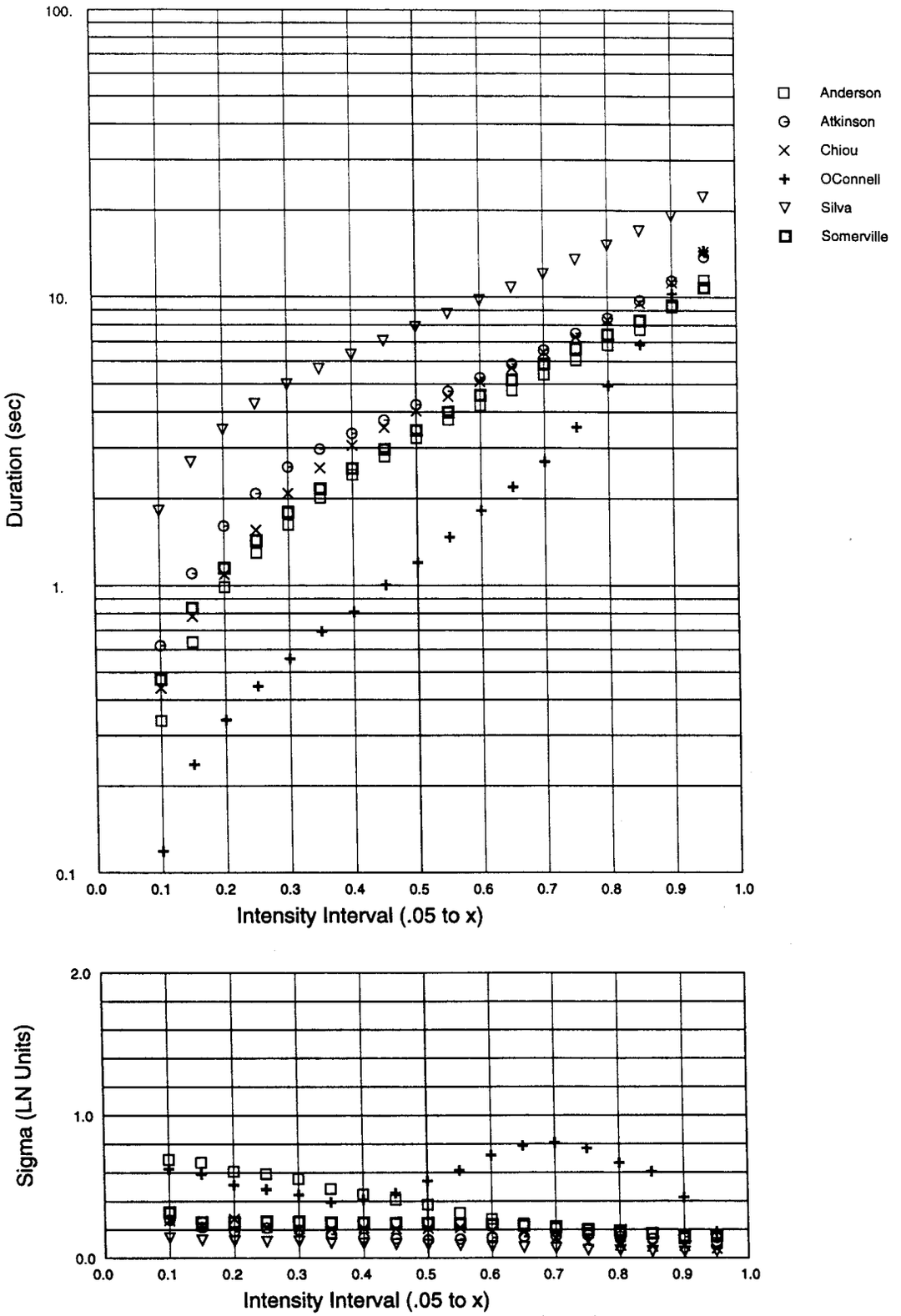

FIGURE 4-6 Scenario Site 1: Acceleration Duration of Horizontal Ground Motions Computed in Scenario Modeling Exercise
(Note: Durations of the average of the two horizontal components are shown.)

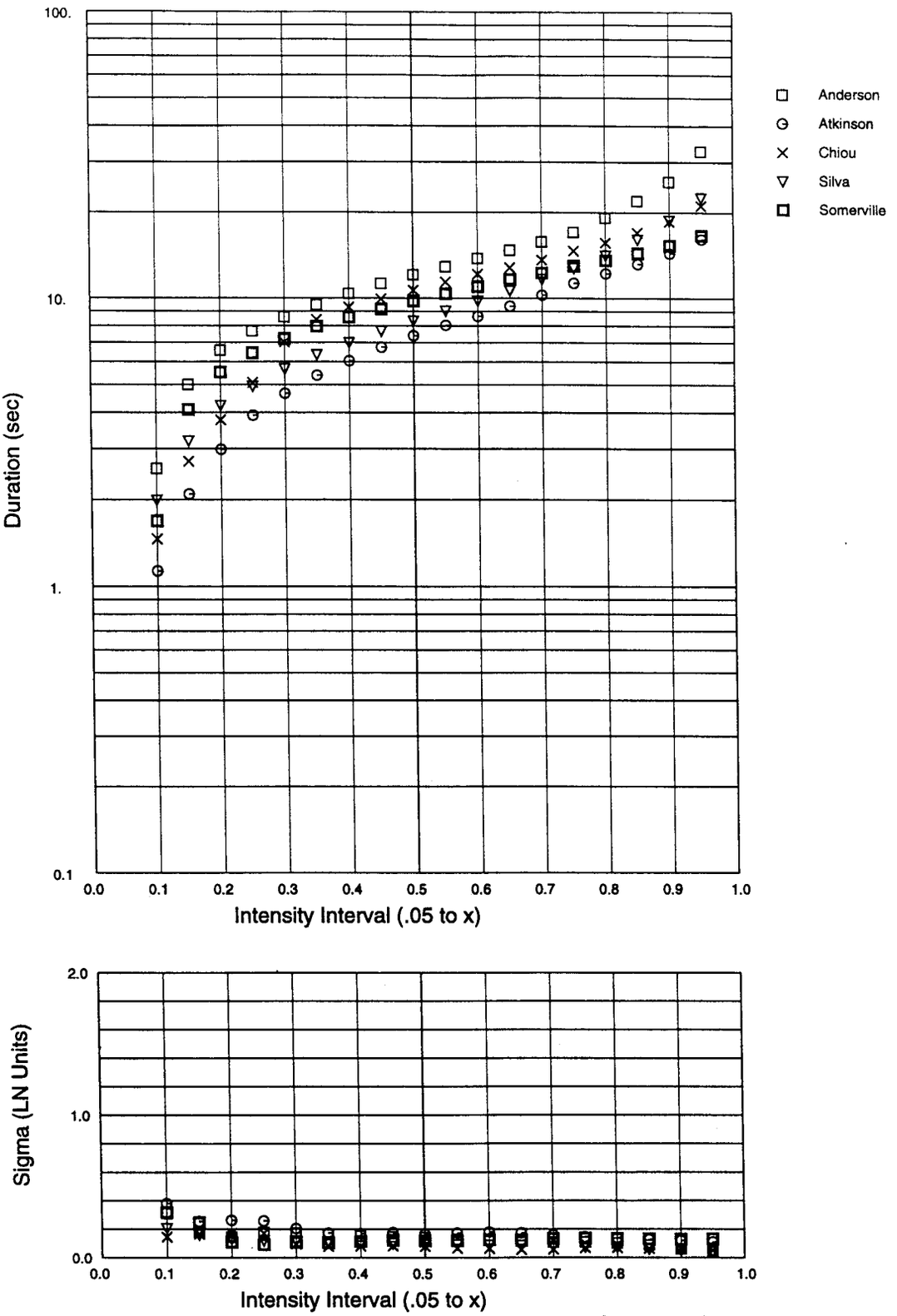

FIGURE 4-7 Scenario Site 21: Acceleration Duration of Horizontal Ground Motions Computed in Scenario Modeling Exercise
(Note: Durations of the average of the two horizontal components are shown.)

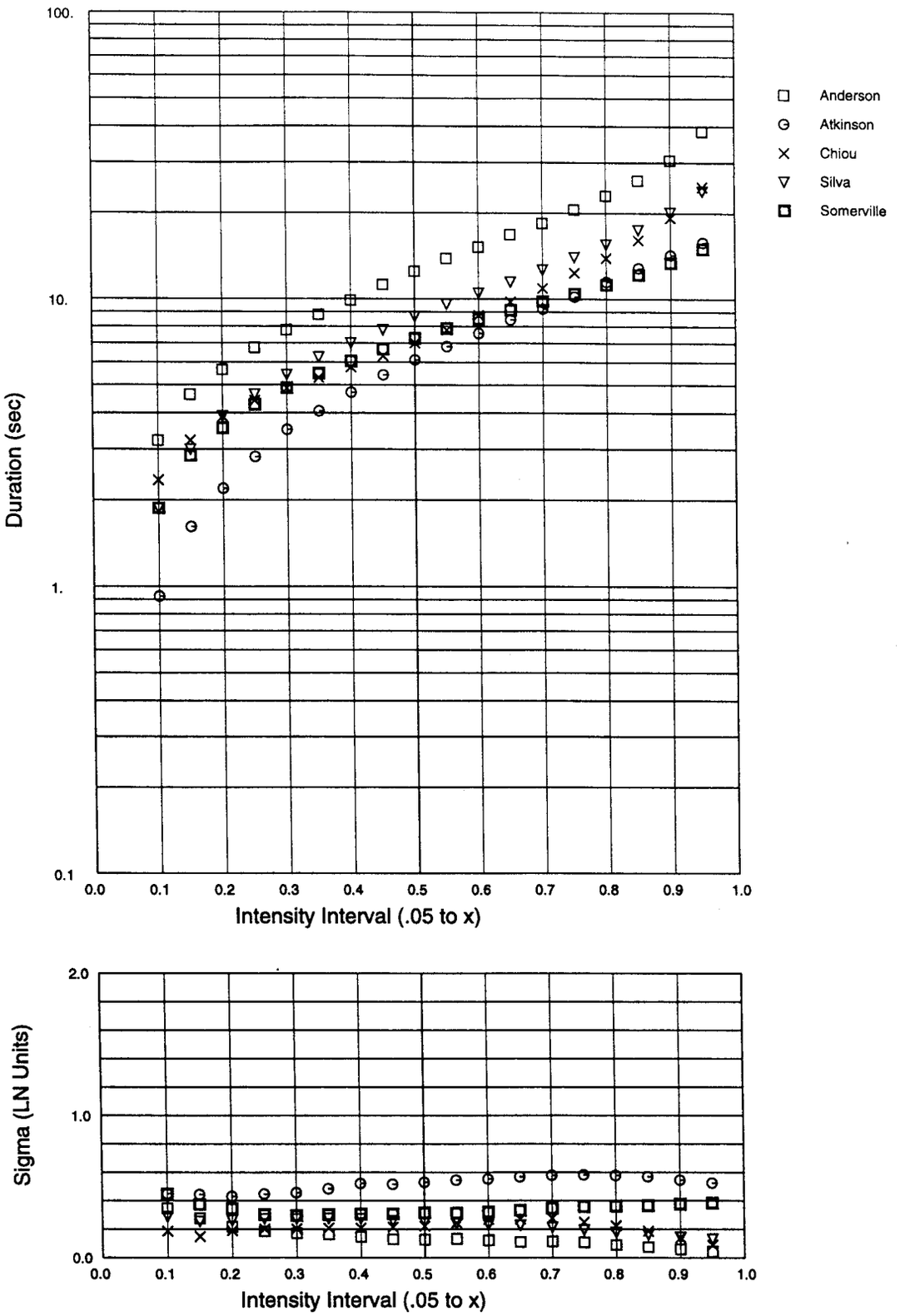

FIGURE 4-8 Scenario Site 29: Acceleration Duration of Horizontal Ground Motions Computed in Scenario Modeling Exercise
(Note: Durations of the average of the two horizontal components are shown.)

SECTION 5
CONCLUSIONS

The root question addressed in the MCEER/FHWA workshop is whether the existing modeling methods may be confidently applied to ENA projects to develop time histories and attenuation relations for engineering analyses. In terms of providing time histories, the methods can produce time histories with reasonable non-stationary characteristics, but they will likely need to be scaled to the design spectral level. Regarding attenuation relations, intuitively, finite fault methods present a better seismological model of the physical process than point source models that are the basis of existing EUS attenuation relations, but additional source parameters required makes these models less robust. Finite fault models will not be ready for use in attenuation relations for ENA until adequate validation is completed. Based on comparisons of the simulated values for all methods, there are differences of up to factors of 5 in amplitude and duration between the different models. There is a wide range in the number of earthquakes against which the methods have been validated - from 1 to 17 earthquakes (Table 3-1). Validation against a standard earthquake data set, with an adequate number of recordings for each earthquake, should significantly reduce this range of model predictions. For example, the range in predictions between those models with more validations varies by about a factor of 3 as compared to a factor of 5 for all the models.

The single-event validation provided an example of the validation process but should not be taken by itself as an evaluation of the models. Some of the models have been shown in other validation exercises to well-match recorded motions on average. A comprehensive series of validations of each model should be performed and thoroughly documented. Taking this to be the case, the workshop provided a valuable forum for proponents of the less well-studied models to begin the validation process.

The variation in simulation results for the models studied is large; however, at high frequencies, the total aleatory variability is larger than the epistemic uncertainty due to different simulation procedures. The epistemic uncertainty and aleatory variability of horizontal spectral acceleration for site 21 lying about 150 km normal to the strike of the fault plane are shown in Figure 5-1. Although the epistemic uncertainty between median ground motions for different methods is much larger than parametric variability within a model, the total aleatory variability (combination of modeling variability and parametric variability) is larger than the epistemic uncertainty. Since the epistemic uncertainty is not dominate except at long periods, this gives some confidence in the use of simulations to predict the distribution of the ground motion for use in engineering applications. Further validations of the methods against a larger data set should help to reduce the epistemic uncertainty.

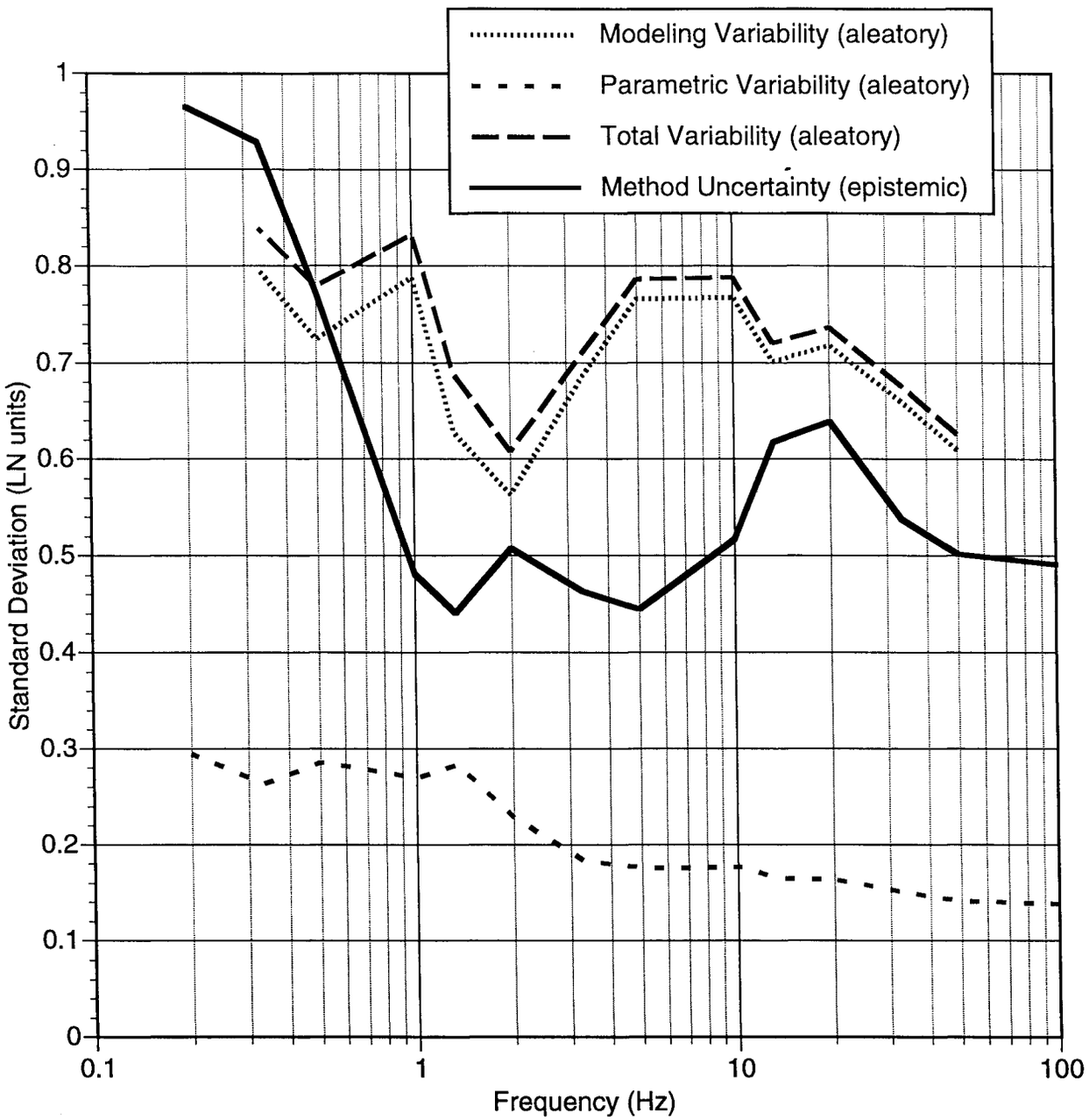

FIGURE 5-1 Comparison of Aleatory Variability and Epistemic Uncertainty Site 21 (Note: At high frequencies, the aleatory variability is larger than the epistemic uncertainty due to the different simulation models.)

The consensus opinion among workshop participants is that model acceptability criteria should be developed which define permissible limits on model bias. Methods that are documented and meet the criteria, using a standard set of validation records archived in a library, could then be objectively identified as adequate for application in the EUS. Participants agreed the validation library should include strong motions from all ENA earthquakes with magnitude greater than 4.5, regardless of recording distance. About ten WUS events should also be included, with magnitudes greater than about 5.5 and motions recorded at distances of less than 100 km.

This type of comprehensive model validation process presents a large task for modelers, but it is a necessary step. Until this is done, unacceptably large differences in simulated ground motions between different modelers will remain.

SECTION 6
REFERENCES

Beresnev, I.A., and G.M. Atkinson (1997), "Modeling Finite-Fault Radiation from the ω^n Spectrum," *Bull. Seism. Soc. Am.*, 87, 67-84.

Beresnev, I.A. and G.M. Atkinson (1998a), "FINSIM - A FORTRAN Program for Simulating Stochastic Acceleration Time Histories from Finite Faults," *Seism. Res. Lett.,* 69, 27-32.

Beresnev, I.A. and G.M. Atkinson (1998b), "Stochastic Finite-Fault Modeling of Ground Motions from the 1994 Northridge, California Earthquake, 1, Validation on Rock Sites," *Bull. Seism. Soc. Am.* (in review).

Beresnev, I.A. and G.M. Atkinson (1998c), "Generic Finite-Fault Model for Ground-Motion Prediction in Eastern North America," submitted to *Bull. Seism. Soc. Am.*

Bernard, P., Herrero, A. and C. Berge (1996), "Modeling Directivity of Heterogeneous Earthquake Ruptures," *Bull. Seism. Soc. Am.*, 86, 1149-1160.

Boatwright, J. and G. Choy (1992), "Acceleration Source Spectra for Large Earthquakes in Northeastern North America," *Bull. Seism. Soc. Am.*, 82, 660-682.

Boore, D.M. (1983), "Stochastic Simulation of High-Frequency Ground Motions Based on Seismological Models of the Radiated Spectra," *Bull. Seism. Soc. Am.,* 73, 1865-1894.

Boore, David M. and Gail M. Atkinson (1992), "Source Spectra for the 1988 Saguenay, Quebec, Earthquakes," *Bull. Seism. Soc. Am.,* 82, 683-719.

Frankel, A. (1991), "High-Frequency Spectral Fall-off for Earthquakes, Fractal Dimension of Complex Rupture, B-value, and the Scaling of Strength on Faults," *J. Geophys. Res.,* 96, 6291-6302.

Haddon, R.A.W. (1992), "Waveform Modeling of Strong-Motion Data for the Saguenay Earthquake of 25 November 1988," *Bull. Seism. Soc. Am.*, 82, 720-754.

Hartzell, S., Langer, C. and C. Mendoza (1994), "Rupture Histories of Eastern North American Earthquakes," *Bull. Seism. Soc. Am.*, 84, 1703-1027.

Herrero, A. and P. Bernard (1994), "A Kinematic Self-Similar Rupture Process for Earthquakes," *Bull. Seism. Soc. Am.*, 83, 1216-1228.

Hutchings, L.J. and F. Wu (1990), "Empirical Green's Functions from Small Earthquakes - A Waveform Study of Locally Recorded Aftershocks of the San Fernando Earthquake," *J. Geophys. Res.*, 95, 1187-1214.

Hutchings, Lawrence (1991), "'Predictions' of Small Ground Motion for the 1989 Loma Prieta Earthquake Using Empirical Green's Functions," *Bull. Seism. Soc. Am.*, 81, 1813-1837.

Hutchings, Lawrence (1994), "Kinematic Earthquake Models and Synthensized Ground Motion Using Empirical Green's Functions," *Bull. Seism. Soc. Am.*, 84, 1028-1050.

Jarpe, S.P. and P.W. Kasameyer (1996), "Validation of a Procedure for Calculating Broadband Strong-Motion Time Histories with Empirical Green's Functions," *Bull. Seism. Soc. Am.*, 86, 1116-1129.

Joyner, W.B. (1995), "Stochastic Simulation of Near-Source Earthquake Ground Motion," *Proceedings of Workshop on Modeling Earthquake Ground Motion at Close Distances*, September 5-6, 1990, EPRI Report EPRI TR-104975.

Luco, J.E. and R.J. Apsel (1983), "On the Green's Functions for a Layered Half Space, Part 1," *Bull. Seism. Soc. Am.,* 73, 909-929.

Silva, W.J. and K. Lee (1987), "WES RASCAL Code for Synthesizing Earthquake Ground Motions," *State of the Art for Assessing Earthquake Hazards in the United States*, Report 24, U.S. Army Waterways Experiment Station, Misc. Paper S-73-1.

Somerville, P.G., McLaren, J.P., Saikia, C.K. and D.V. Helmberger (1990), "The 25 November 1988, Quebec, Earthquake: Source Parameters and the Attenuation of Strong Ground Motion," *Bull. Seism. Soc. Am.*, 80, 1118-1143.

Somerville, P.G. (1993), "Engineering Applications of Strong Ground Motion Simulation," *Tectonophysics*, 218, 195-219.

Su, Feng, Anderson, John G., Brune, James N. and Yuehua Zeng (1996), "A Comparison of Direct S-Wave and Coda Wave Site Amplification Determined from Aftershocks of the Little Skull Mountain Earthquake," submitted for publication to *Bull. Seism. Soc. Am.,* Feb. 5.

Zeng, Y. and J.G. Anderson (1994), "A Method for Direct Computation of the Differential Seismogram with Respect to the Velocity Change in a Layered Elastic Solid," *Bull. Seism. Soc. Am.,* 73, 909-929.

Zeng, Y., Anderson, J.G. and F. Su (1995), "Subevent Rake and Random Scattering Effects in Realistic Strong Ground Motion Simulation," *Geophys. Res. Lett.,* 22, 17-20.

Zeng, Y., Anderson, J.G. and G. Yu (1994), "A Composite Source Model for Computing Realistic Synthetic Strong Ground Motions," *Geophys. Res. Lett.,* 21, 725-728.

Appendix A
Workshop Information

Workshop Program

Workshop Participants

Instructions to Workshop Participants

MCEER Workshop on Ground Motion Methodologies for the Eastern United States
Sheraton Four Points Hotel,
Memphis, Tennessee
October 16 and 17, 1999

AGENDA

Thursday, October 16

8:30 Registration and Continental Breakfast - *Conference Room 5*

9:00 Welcome and Introduction (Friedland)

9:15 Objective of Workshop (Abrahamson)

9:30 Engineering User Needs (Power)

9:45 Review of Exercises (Abrahamson)

10:00 Treatment of Uncertainty and Model Validation (Abrahamson)

10:15 Break

Summary of Modeling Methodologies and Validations
10:30 Anderson
10:55 Chiou
11:20 Silva
11:45 Somerville

12: 10 Lunch - *Conference Room 4*

Summary of Modeling Methodologies (continued)
1:10 Hutchings/Jarpe
1:35 O'Connell
2:00 Atkinson
2:25 Papagoriou

2:50 Break

3:10 Results of Validation Exercise (Abrahamson)

4:00 Discussion
Validations for other events?
Are the methods adequately validated?

4:30 Comments From Users

5:00 Adjourn

Friday, October 17

8:30 Gathering and Continental Breakfast - *Conference Room 5*

9:00 Comparison of Results of Simulation Exercise (Abrahamson)
Comparisons of ground motion parameters and waveforms

10:00 Discussion of Simulation Results

10:30 Break

10:45 Discussion of Simulation Results (continued)

11:15 Simulation Issues (Abrahamson)
How to evaluate the reasonableness of time histories?
What should be the criteria - duration, peak velocity, peak displacement, Arias Intensity?

12:00 Lunch - *Conference Room 4*

1:00 Engineering Application of Ground Motion Simulations
Comments from users.
Need for a library of "MCEER approved" time histories?
How should the time histories be scaled?

2:00 Consensus Recommendations for Ground Motion Modeling (Abrahamson)

3:30 Adjourn

MCEER Workshop on Ground Motion Methodologies for the Eastern United States
Sheraton Four Points Hotel,
Memphis, Tennessee
October 16 and 17, 1999

PARTICIPANTS
(Last Updated October 13, 1997)

Norman A. Abrahamson
Engineering Seismology Consultant
152 Dracena Avenue
Piedmont, CA 94611
(510) 428-9823 (phone)
(510) 428-9824 (fax)
nabraham@holonet.net

John G. Anderson
Seismological Laboratory, MS 174
University of Nevada, Reno
Reno NV, 89557
(702) 784-4265 (phone)
(702) 784-1833 (fax)
jga@seismo.unr.edu

Seraftm G. Arzoumanidis, P.E.
Technical Director Special Projects
Steinman Boynton Gronquist &
Birdsall
110 William Street
New York, NY 10038
(212) 266-8370 (phone)
(212) 266-8540 (fax)
serafim_g_arzoumanidis@parsons.com

Gail M. Atkinson
Department of Earth Sciences
Carleton University, 304 Tory Building
1125 Colonel By Drive
Ottawa, Ontario K1S 5B6
CANADA
(613) 520-2600 ext 1399 (phone)
(613) 520-4490 (fax)
gma@ccs.carleton.ca

Igor A. Beresnev
Department of Earth Sciences
Carleton University, 304 Tory Building
1125 Colonel By Drive
Ottawa, Ontario K1S 5B6
CANADA
(613) 520-2600 ext 1393 (phone)
(613) 520-4490 (fax)
beresnev@ccs.carleton.ca

Shyh-Jeng Chiou
Project Seismologist
Geomatrix Consultants, Inc.
100 Pine Street, 10th Floor
San Francisco, CA 94111
(415) 434-9400 (phone)
(415) 434-1365 (fax)
sjchiou@geomatrix.com

Arthur Frankel
U.S. Geological Survey
P.O. Box 25046, MS 966
Denver Federal Center
Denver, CO 80225
(303) 273-8556 (phone)
(303) 273-8600 (fax)
afrankel@usgs.gov

Ian M. Friedland, P.E.
Applied Technology Council
1300 Pennsylvania Ave. NW
Suite 700
Washington, D.C.
(202) 204-3011 (phone)
(202) 204-3012 (fax)
ifriedland@atcouncil.org

Lawrence Hutchings
Lawrence Livermore National Lab.
Earth Sciences Department, L-208
PO Box 808
Livermore, CA 94550
(510) 423-0354 (phone)
(510) 422-3925 (fax)
hutchings2@llnl.gov

I.M. Idriss
Professor, Civil Engineering Dept.
University of California at Davis
P.O. Box 330
Davis, CA 95617
(916) 752-5403 (phone)
(916) 758-1104 (fax)

Manouchehr Karshenas, S.E., P.E.
Special Design and Evaluation Engr.
Illinois Department of Transportation
Bureau of Bridges and Structures
2300 Dirksen Parkway
Springfield, IL 62764
(217) 785-3054 (phone)
(217) 782-7960 (fax)
karshenasmj@nt.dot.state.il.us

W. David Liu
Technical Director
Imbsen & Associates, Inc.
9912 Business Park Drive, Suite 130
Sacramento, CA 95827
(916) 366-0632 (phone)
(916) 366-1501 (fax)
wdliu@imbsen.com

Ayaz H. Malik
Project Engineer - Structures Division
New York State Dept. of Transp.
1220 Washington Avenue, B5-600
Albany, NY 12232
(518) 457-6465 (phone)
(518) 485-7826 (fax)
amalik@gw.dot.gov.state.ny.us

Shean-Der Ni
Graduate Assistant
Seismological Laboratory, MS 174
University of Nevada, Reno
Reno, NV 89557
(702) 784-4263
(702) 784-1833
sdni@seismo.unr.edu

Daniel R. H. O'Connell
U.S. Bureau of Reclamation
Denver Federal Center
P.O. Box 25007, D-8330
Denver, CO 80225-0007
(303) 236-4195 ext 275 (phone)
(303) 236-9127 (fax)
geomagic@seismo.usbr.gov

Apostolos S. Papageorgiou
Dept. of Civil, Structural and
Environmental Engineering
University at Buffalo,
State University of New York
222 Ketter Hall
Buffalo, NY 14261
(716) 645-2114 ext 2416 (phone)
(716) 645-3733 (fax)
ap23@eng.buffalo.edu

Henry Pate
Tennessee Dept. of Transportation
James K. Polk Building, Suite 1100
505 Deaderick Street
Nashville, TN 37243-0339
(615) 741-8295 (phone)
(615) 532-7745 (fax)

Joseph Penzien, Chairman
International Civil Engineering
Consultants, Inc.
1995 University Avenue, Suite 119
Berkeley, CA 94704
(510) 841-7328 (phone)
(510) 841-7438 (fax)
cec@icec.com

Shahram Pezeshk, P.E.
The University of Memphis
Department of Civil Engineering
Campus Box 526570
Memphis, TN 38152
(901) 678-4727 (phone)
(901) 678-3026 (fax)
s-pezeshk@memphis.edu

Maurice S. Power
Geomatrix Consultants, Inc.
100 Pine Street, 10th Floor
San Francisco, CA 94111
(415) 434-9400 (phone)
(415) 434-1365 (fax)
cmusacchia@geomatrix.com

Walter Silva
Pacific Engineering and Analysis
311 Pomona Avenue
El Cerrito, CA 94530
(510) 528-2821 (phone)
(510) 528-2135 (fax)
pacific@crl.com

Paul Somerville
Senior Consulting Seismologist
Woodward-Clyde Federal Services
566 El Dorado Street, Suite 100
Pasadena, CA 91101-2560
(818) 449-7650 (phone)
(818) 449-3536 (fax)
pgsomero@wcc.com

Gabriel R. Toro
Vice President
Risk Engineering Inc.
4155 Darley Avenue, Suite A
Boulder, CO 80303
(303) 499-3000 (phone)
(303) 499-4850 (fax)
toro@riskeng.com

Houston Walker
Tennessee Dept. of Transportation
James K. Polk Building, Suite 1100
505 Deaderick Street
Nashville, TN 37243-0339
(615) 741-7621 (phone)
(615) 532-7745 (fax)

Workshop on Ground Motion Methodologies for the Eastern United States
FHWA/MCEER Highway Project Task 106-F-5.4.2

INSTRUCTIONS TO PARTICIPANTS

Objective:

The objective of this two-day workshop is to evaluate the current methods for developing rock time histories for engineering applications in the Eastern United States (EUS). There are two issues to consider in this regard: the amplitude of the ground motion (e.g. response spectra) and the character of the time history. The following questions will be addressed during the workshop: Which methods can be used to reliably predict the amplitude of the ground motion (median and variability) for defining design spectra? Which methods can be used to define the non-stationary characteristics of the time history? Should time histories be scaled? If so, what are the scaling rules? How can the results of the simulated time histories be evaluated to ensure that they are reasonable?

Approach:

To allow an evaluation of various models and methodologies, both a validation exercise and a simulation exercise will be conducted. These exercises will be performed by each of the ground motion modelers using their proposed methods and models. The results of the exercises will be submitted by each modeler to Dr. Norman Abrahamson prior to the workshop so that they can be evaluated and presented in a standardized format for use during the workshop.

1. Validation Exercise

The validation is intended to evaluate how well the models can predict the ground motion from previously recorded earthquakes. The comparisons will be made for response spectral values, peak velocity, peak displacement, and duration. Ideally, this validation exercise should include a large number of earthquakes; however, that is beyond the scope of this workshop. For this workshop, only a single event validation is being requested.

There are two moderate-to-large events available for the EUS: the 1988 Saguenay earthquake, and the 1985 Nahanni earthquake. The Saguenay event is the best recorded EUS event with M>5 (distances 40-150 km), but it may have an anomalous source. The Nahanni event has closer distances (8-16 km) with a larger magnitude, but it did not occur in the EUS (although the spectral content looks like EUS ground motion).

For this exercise, the Saguenay event has been selected. A drawback to this selection is that many seismologists consider it to be anomalous. This begs the question that if a model produces a good match to Saguenay, will that model then produce a poor match for other more

typical earthquakes? To help address this, if a model has been validated against other earthquakes, that information should be provide by the modeler as well.

The following stations from Saguenay should be modeled:

Code	Station Name	Dist (km)	Code	Station Name	Dist (km)
SM01	St. Ferreol, Quebec	114	SM10	Riviere-Quelle, Quebec	114
SM02	Quebec, Quebec	150	SM16	Chicoutimi-Nord, Quebec	48
SM05	Tadoussac, Quebec	110	SM17	St-Andre-du-Lac-St-Jean	66
SM08	La Malbaie, Quebec	94	SM20	Les Eboulements, Quebec	91
SM09	St-Pascal, Quebec	123			

From the validation exercise, the bias of each model will be evaluated (i.e., is the model adequate on average?) along with the variability of the residuals of the model predictions. This is needed to define the total standard deviation of the prediction. (If validations from a larger number of events have already been computed, modelers should include these results as well).

2. Simulation

The simulation exercise is not for a specific location. The event parameters are given below:

Site condition: hard rock, kappa = 0.006 sec
Moment magnitude: 7.0 (moment = 3.55 E26 dyne-cm)
Dip: 45 degrees (E)
Strike: 0
Rake: 90
Dimension: 50 km x 20 km
Top of fault: 2 km
Velocity structure: EPRI Midcontinent model
Distances: 0 - 500 km
Source realizations: (as appropriate for each model)

Each of the source parameters that were optimized in the validation exercise should be varied in this simulation. This may include the following: slip model, hypocenter location, sub-event parameters. A minimum of 10 source realizations should be run to define the parametric variability term (30 is better, but 10 is sufficient for this workshop).

Fault Coordinates: (x, y, z) in km

Top of fault: (0,25,2) (0,-25,2)
Bottom of fault: (14.14,25,16.14) (14.14,-25,16.14)

Appendix B
Model Validation Against Saguenay Earthquake

The plots in this Appendix document the model validations against the recorded motions of the Saguenay earthquake. Each modeler participating in the validation exercise provided horizontal acceleration time histories computed at nine Saguenay recording sites (Table 3-2). The acceleration histories were subsequently integrated for velocity and displacement. The time histories are shown in Figures B-1.1 through B-1.27. The recorded Saguenay motion and the synthetic motions are plotted for each recording station. The modeler, trace designation, and peak trace amplitude are listed to the right of each trace.

Spectra and acceleration durations were computed from the acceleration histories; velocity and displacement durations were computed from the integrated motions. The spectral accelerations are plotted in Figures B-2.1 through B-2.9 and the durations in Figures B-3.1 through B-3.27.

Three of the participants provided vertical motions. The vertical time histories, spectra, and durations are shown in Figures B-4.1 through B-4.27, B-5.1 through B-5.9, and B-6.1 through B-6.27.

The figures are provided on MCEER's web site at http:/mceer.buffalo.edu. From the home page, select "Publications," then "Interactive Catalog." A search form will appear. Enter 99-0016 under the publication number on the form and select "Search." Follow the instructions on screen to locate and download the supplementary files.

Appendix C
Anderson Scenario Modeling Results

The plots in this Appendix document the synthetic seismograms developed by Anderson and Ni in the scenario modeling exercise. Three sets of figures are supplied: the first is the east component of motion (Figures C-1.1 through C-1.30), the second is the north component (Figures C-2.1 through C-2.30), and the last is the vertical component (Figures C-3.1 through C-3.30). Anderson and Ni provided 10 synthetic accelerograms at each of the 30 scenario stations. All 10 realizations at a station are plotted together on a single page. Eighty seconds of motion are printed. To the right of each accelerogram are printed the peak trace amplitude in *g* and the name of the file as supplied by Anderson and Ni.

The figures are provided on MCEER's web site at http:/mceer.buffalo.edu. From the home page, select "Publications," then "Interactive Catalog." A search form will appear. Enter 99-0016 under the publication number on the form and select "Search." Follow the instructions on screen to locate and download the supplementary files.

Appendix D
Atkinson Scenario Modeling Results

The plots in this Appendix document the synthetic seismograms developed by Atkinson and Beresnev in the scenario modeling exercise. One set of figures is supplied for an average horizontal component of motion (Figures D-1.1 through D-1.30). Atkinson and Beresnev provided 10 synthetic accelerograms at each of the 30 scenario stations. All 10 realizations at a station are plotted together on a single page. Eighty seconds of motion are plotted. To the right of each accelerogram are printed the peak trace amplitude in *g* and the name of the file as supplied by Atkinson and Beresnev.

The figures are provided on MCEER's web site at http:/mceer.buffalo.edu. From the home page, select "Publications," then "Interactive Catalog." A search form will appear. Enter 99-0016 under the publication number on the form and select "Search." Follow the instructions on screen to locate and download the supplementary files.

Appendix E
Chiou Scenario Modeling Results

The plots in this Appendix document the synthetic seismograms developed by Chiou in the scenario modeling exercise. Three sets of figures are supplied: two horizontal components of motion (HI and H2; Figures E-1.1 through E-1.50 and E-2.1 through E-2.50, respectively) and a vertical component of motion (Figures E-3.1 through E-3.50). Chiou provided 12 synthetic accelerograms at 25 of the 30 scenario stations (all except Stations 11, 12, 23, 24, and 30). The realizations at a station are plotted 10 per page. Eighty seconds of motion are plotted. To the right of each accelerogram are printed the peak trace amplitude in *g* and the name of the file as supplied by Chiou.

The figures are provided on MCEER's web site at http:/mceer.buffalo.edu. From the home page, select "Publications," then "Interactive Catalog." A search form will appear. Enter 99-0016 under the publication number on the form and select "Search." Follow the instructions on screen to locate and download the supplementary files.

Appendix F
O'Connell Scenario Modeling Results

The plots in this Appendix document the synthetic seismograms developed by O'Connell in the scenario modeling exercise. Three sets of figures are supplied: two horizontal components of motion (east and north; Figures F-1.1 through F-1.30 and F-2.1 through F-2.30, respectively) and a vertical component of motion (Figures F-3.1 through F-3.30). O'Connell provided 30 synthetic accelerograms at 10 of the 30 scenario stations (Stations 1, 2, 3, 4, 13, 14, 15, 16, 25, and 26). The realizations at a station are plotted 10 per page. Eighty seconds of motion are plotted. To the right of each accelerogram are printed the peak trace amplitude in *g* and the name of the file as supplied by O'Connell.

The figures are provided on MCEER's web site at http:/mceer.buffalo.edu. From the home page, select "Publications," then "Interactive Catalog." A search form will appear. Enter 99-0016 under the publication number on the form and select "Search." Follow the instructions on screen to locate and download the supplementary files.

Appendix G
Silva Scenario Modeling Results

The plots in this Appendix document the synthetic seismograms developed by Silva in the scenario modeling exercise. A single set of figures is supplied for an average horizontal component of motion (Figures G-1.1 through G-1.90). Silva provided 30 synthetic accelerograms at all 30 scenario stations. The realizations at a station are plotted 10 per page. Eighty seconds of motion are plotted. To the right of each accelerogram are printed the peak trace amplitude in *g* and the name of the file as supplied by Silva.

The figures are provided on MCEER's web site at http:/mceer.buffalo.edu. From the home page, select "Publications," then "Interactive Catalog." A search form will appear. Enter 99-0016 under the publication number on the form and select "Search." Follow the instructions on screen to locate and download the supplementary files.

Appendix H
Somerville Scenario Modeling Results

The plots in this Appendix document the synthetic seismograms developed by Somerville in the scenario modeling exercise. Three sets of figures are supplied: two horizontal components of motion (east and north, Figures H-1.1 through H-1.78 and Figures H-2.1 through H-2.78, respectively) and the vertical component (Figures H-3.1 through H-3.78). Somerville provided 27 synthetic accelerograms at 26 of the 30 scenario stations (all except Stations 11, 12, 23, and 24). The realizations at a station are plotted 10 per page. Eighty seconds of motion are plotted. To the right of each accelerogram are printed the peak trace amplitude in *g* and the name of the file as supplied by Somerville.

The figures are provided on MCEER's web site at http:/mceer.buffalo.edu. From the home page, select "Publications," then "Interactive Catalog." A search form will appear. Enter 99-0016 under the publication number on the form and select "Search." Follow the instructions on screen to locate and download the supplementary files.

Appendix I
Horizontal Synthetic Motion Summaries

The plots in this Appendix compare the results of the scenario modeling of horizontal ground motion for all modelers at the 30 scenario stations. Response spectra and time history durations were computed for an average horizontal component of motion - the results plotted are geometric means of both horizontal components of motion (or one if only an average component were provided) for all realizations provided by each modeler. Four sets of plots are provided: spectral acceleration (Figures I-1.1 through I-1.30), acceleration duration (Figures I-2.1 through I-2.30), velocity duration (Figures I-3.1 through I-3.30), and displacement duration (Figures I-4.1 through I-4.30). The standard deviations of the values are also shown.

The figures are provided on MCEER's web site at http:/mceer.buffalo.edu. From the home page, select "Publications," then "Interactive Catalog." A search form will appear. Enter 99-0016 under the publication number on the form and select "Search." Follow the instructions on screen to locate and download the supplementary files.

Appendix J
Vertical Synthetic Motion Summaries

The plots in this Appendix compare the results of the scenario modeling of vertical ground motion for all modelers at the 30 scenario stations. Response spectra and time history durations were computed for the vertical components of motion provided by each modeler - the results plotted are geometric means for all realizations. Four sets of plots are provided: spectral acceleration (Figures J-1.1 through J-1.30), acceleration duration (Figures J-2.1 through J-2.30), velocity duration (Figures J-3.1 through J-3.30), and displacement duration (Figures J-4.1 through J-4.30). The standard deviations of the values are also shown.

The figures are provided on MCEER's web site at http:/mceer.buffalo.edu. From the home page, select "Publications," then "Interactive Catalog." A search form will appear. Enter 99-0016 under the publication number on the form and select "Search." Follow the instructions on screen to locate and download the supplementary files.

MULTIDISCIPLINARY CENTER FOR EARTHQUAKE ENGINEERING RESEARCH

A National Center of Excellence in Advanced Technology Applications

University at Buffalo, State University of New York
Red Jacket Quadrangle ▪ Buffalo, New York 14261-0025
Phone: 716/645-3391 ▪ Fax: 716/645-3399
E-mail: mceer@acsu.buffalo.edu ▪ WWW Site: http://mceer.buffalo.edu